

AD-A047 303

RAYTHEON CO PORTSMOUTH R I SUBMARINE SIGNAL DIV  
PARAMETRIC SONAR STUDY NEAR-FIELD INVESTIGATION, (U)  
JUL 77 J C LOCKWOOD

F/G 17/1

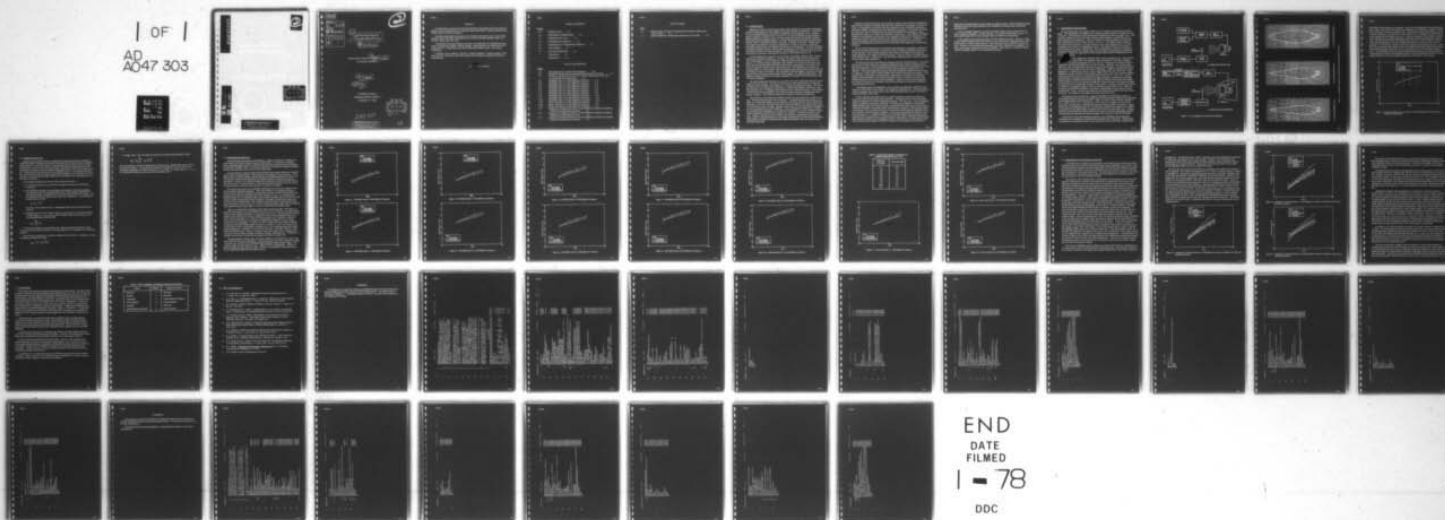
UNCLASSIFIED

R1706

N00024-76-C-6051

NL

| OF |  
AD  
A047 303



AD A 0 4 7 3 0 3

2  
B.S.

AD No. \_\_\_\_\_  
DDC FILE COPY

DDC  
RECEIVED  
DEC 6 1977  
RESERVED  
D

DISTRIBUTION STATEMENT A  
Approved for public release;  
Distribution Unlimited

14 R1706

ACCESSION for	
NTIS	White Section <input checked="" type="checkbox"/>
DDC	Bufi Section <input type="checkbox"/>
UNANNOUNCED	<input type="checkbox"/>
JUSTIFICATION	
Per Hs on file	
BY	
DISTRIBUTION/AVAILABILITY CODES	
Dist.	AVAIL. and/or SPECIAL
A	

6  
PARAMETRIC SONAR STUDY  
NEAR-FIELD INVESTIGATION

10  
Dr. James C. Lockwood

15  
Prepared under Contract No. N00024-76-C-6051  
for NAVSEA Code 06H1-1

11  
29 July 1977

12 49p.

RAYTHEON COMPANY  
SUBMARINE SIGNAL DIVISION  
Portsmouth, RI 02871

DDC  
RECEIVED  
DEC 6 1977  
4 D

298 125

DISTRIBUTION STATEMENT A  
Approved for public release;  
Distribution Unlimited

1B

## PREFACE

The opportunity to perform this Nearfield Parametric Sonar Study was made possible by adding a series of measurements to a Special Purpose Sonar (SPS) Transducer Measurement Program that was already in progress.

Nearfield measurements were made at the Transducer Evaluation Center, Naval Ocean Systems Center, San Diego, California and at the Naval Underwater Systems Center Test Facility, Seneca Lake, New York.

I am grateful to the help extended to me both in collecting data and critiquing this report by Dr. George Walsh, Messrs. William Backman, James Bartram, and Dennis McCrady of Raytheon; and Dr. Mark Moffet of the Naval Underwater Systems Center, New London, Connecticut.

In addition I wish to thank Mr. Herbert C. Single of Raytheon, Program Manager of this study, and Mr. John Neely, Code 06H1 NAVSEA, who authorized and funded the work that was performed.

Dr.  C. Lockwood



## TABLE OF CONTENTS

Section

1.0	INTRODUCTION . . . 1-1
2.0	EXPERIMENT DESCRIPTIONS . . . 2-1
3.0	CORRECTION OF DATA . . . 3-1
4.0	EXPERIMENTAL RESULTS . . . 4-1
5.0	COMPARISON OF THEORETICAL RESULTS . . . 5-1
6.0	CONCLUSIONS . . . 6-1
7.0	LIST OF REFERENCES . . . 7-1
	APPENDIX A . . . A 1
	APPENDIX B . . . B 1

## LIST OF ILLUSTRATIONS

Figure

2-1	Test Configuration Functional Block Diagrams . . . 2-2
2-2	TRANSDEC Beampatterns Demonstrating Intermodulation Distortion . . . 2-3
2-3	Secondary Frequency Source Level at 1.5 kHz as Measured for Four Drive Levels (Seneca Lake Experiment) . . . 2-4
4-1	TRANSDEC Data at 1.0 kHz Difference Frequency . . . 4-2
4-2	TRANSDEC Data at 1.5 kHz Difference Frequency . . . 4-2
4-3	TRANSDEC Data at 2.0 kHz Difference Frequency . . . 4-3
4-4	TRANSDEC Data at 2.5 kHz Difference Frequency . . . 4-3
4-5	TRANSDEC Data at 3.0 kHz Difference Frequency . . . 4-4
4-6	TRANSDEC Data at 4.0 kHz Difference Frequency . . . 4-4
4-7	TRANSDEC Data at 6.0 kHz Difference Frequency . . . 4-5
4-8	TRANSDEC Data at 8.0 kHz Difference Frequency . . . 4-5
4-9	TRANSDEC Data at 10.0 kHz Difference Frequency . . . 4-6
4-10	TRANSDEC Data at 12.0 kHz Difference Frequency . . . 4-6
4-11	Seneca Lake Data at 1.5 kHz Difference Frequency . . . 4-7
4-12	Seneca Lake Data at 2.5 kHz Difference Frequency . . . 4-8
4-13	Seneca Lake Data at 3.0 kHz Difference Frequency . . . 4-8
5-1	Comparison of Theoretical Data for 1.5 kHz Difference Frequency (Conditions of Seneca Lake Experiment Assumed) . . . 5-2
5-2	Comparison of Theoretical Data for 3.0 kHz Difference Frequency (Conditions of Seneca Lake Experiment Assumed) . . . 5-3
5-3	Comparison of Theoretical Data for 10.0 kHz Difference Frequency (Conditions of Seneca Lake Experiment Assumed) . . . 5-3

## LIST OF TABLES

Table

4-1	Measured Data Increases to Compensate for Assumed Constant Mean Source Level . . . 4-7
6-1	Degree of Difficulty and Equipment Required for Each Model . . . 6-2



## 1.0 INTRODUCTION

Difference frequency sound pressure levels in the nearfield of a parametric transmitting array have been measured in two separate experiments with the same projector. The projector has a nearfield distance at the primary frequencies of approximately 6.0 m. Measurements were made at ranges of from 3.0 to 24.0 m, in order to show the nearfield buildup of apparent difference frequency source level from within the projector's nearfield to approximately four times its nearfield distance. The first experiment took place at the Naval Ocean Systems Center's TRANSDEC facility in San Diego, California in July 1976. Measurements were made at ten difference frequencies ranging from 1.0 kHz to 12.0 kHz. In these and succeeding measurements, the projector was driven at two frequencies. The lower frequency remained a constant 42.58 kHz, and the higher frequency was varied from 43.58 to 54.58 kHz to produce the desired difference frequency. The downshift ratio, defined as the ratio of the mean primary frequency to the difference frequency, varied from 43.08 to 4.05.

The data obtained at a range of 24.0 m and some of the higher-frequency data at shorter ranges were considered satisfactory. However, the shorter-range, lower-frequency data were contaminated by receiver distortion, which was apparent from the shape of the beam-patterns. It is believed that the hydrophone used, because it is of the electrostrictive type, has an inherent intermodulation distortion response that is proportional to the square of the primary frequency pressure at the measurement point. If the dependence on primary frequency pressure is in fact quadratic, then the distortion level must increase at a rate of 40.0 dB per decade as range is decreased. Thus a hydrophone showing negligible distortion at ranges greater than 24.0 m may be totally unusable at short ranges or at large downshift ratios. This suggests a fundamental limit to the useful combination of downshift ratios and nearfield range for a given hydrophone.

The second experiment took place in April 1977 at the Naval Underwater Systems Center's Seneca Lake Test Facility. The objective of the Seneca Lake experiment was to repeat the conditions of the TRANSDEC experiment and to overcome the distortion problem. The distortion was hoped to be eliminated by substitution of a different hydrophone, preferably, a non-electrostrictive one. If changing the hydrophone failed to resolve the problem, it was planned to cover the face of the hydrophone with a sound absorbing material to attenuate the intense primary radiation. The distortion would then be expected to diminish quadratically.

The objective of overcoming the distortion problem was not realized for a number of reasons. The major obstacle was a lack of test time. The nearfield measurements were to be taken as a low-priority addition to a test program in which the emphasis was on farfield measurements. In the end, only about three hours became available for nearfield measurements out of over three weeks of testing. Because of lack of time, it was not possible to attempt the use of a sound absorber to cut the distortion. It was not possible to obtain use of a suitable non-electrostrictive hydrophone, so the best that could be done was to use a different electrostrictive hydrophone and hope that it would be less nonlinear. Such did not prove to be the case. However, because time was so short it was decided to concentrate on taking axial levels and not to take beampatterns for all ranges and frequencies as was done at TRANSDEC. Consequently, the degree to which distortion affected the Seneca Lake test results was not determined until later.

Because no distortion-free data set was obtained, efforts were directed at evaluating the data that were obtained to establish which data were reliable and see if the data could be corrected. It was apparent for example, that the beampatterns from TRANSDEC revealed by their shape whether a substantial amount of distortion was present. It was further noted that the signal level could be estimated from the distorted beampatterns by fairing in a more characteristic shape in the vicinity of the maximum response axis. The method of identifying distortion and estimating corrections from the beampattern shape was not regarded as very satisfactory because it relied too heavily on the judgment of the observer. Furthermore, it could not be applied to the data taken at Seneca Lake because patterns were not made. Methods of estimating the distortion level and correcting the data analytically were therefore examined.

By use of the assumptions that the distortion level dependence is quadratic, and that the distortion and signal add in phase, it has been possible to deduce the distortion levels and to correct the data. The corrections depend to some extent on assumptions made about the range dependence of the signal as predicted by theory. However, there is no reliance on predicted absolute levels. Furthermore, only the shortest range data point is seriously affected by the assumed range dependence.

The data from the two experiments are compared with two nearfield theories. Then these two and several other theories are compared among themselves and their similarities and differences are noted. The first published theoretical treatment of the parametric array nearfield was included in the more general numerical volume integration model of Muir and Willette<sup>1</sup>. The volume integration program originally developed by Willette has been revised by Lockwood to include finite-amplitude effects and to improve numerical convergence. In its modified form, the program was used by Muir, Mellenbruch and Lockwood<sup>2</sup> to model the unusual nearfield geometry of the reflected parametric array. Lockwood's version of the Willette program is used in the present investigation. However, for the cases considered, the results are believed to be identical to those that would have been obtained had Willette's original program been used.

An analytical model of the parametric array nearfield was published by Berkday<sup>3</sup> in the same year (1972) that the Muir-Willette work appeared in published form. Because Berkday's model is applicable only to parametric arrays with collimated primary waves, it will not be considered further in this work.

In 1974, Bartram and Fugitt<sup>4</sup> reported a simple closed-form model for a parametric array with conical piston beam primary radiations. Assumptions used in that work include neglect of absorption and of finite-amplitude attenuation. The same year, a more complicated analytical model was reported by Lockwood<sup>5</sup>. Presented as an adaptation of the (farfield) Mellen-Moffett<sup>6</sup> model, the Lockwood model uses geometrically derived correction factors to modify the amplitudes of secondary signals emanating from ranges for which nearfield effects are important. The correction factors are derived under the assumption of negligible losses in the interval to which the factor is applied. Losses occurring outside that interval are properly accounted for. A significant feature of the Lockwood model is that it accounts for the transition from a conical beam to a cylindrical beam at the primary frequency nearfield limit. Other models are based on the assumption of either a cylindrical or a conical primary beam. (The Bartram<sup>4</sup> model contains a cylindrical nearfield in its formulation, but its effect is



suppressed in an approximation used to obtain the reported result.) Both the Bartram and the Lockwood models have been evaluated for the conditions of the Seneca Lake experiments reported herein.

In 1975, Rolleigh<sup>7</sup> published a nearfield model that includes explicit account of the primary frequency beampattern. In other respects, it is similar to the Bartram<sup>4</sup> model. Its major shortcoming is that it does not apply within the nearfield of the projector.

In two recent works, nearfield absorption has been taken into account. The first, a 1975 work of Mellen<sup>8</sup> actually contains two models, one for cylindrically collimated primary waves and the other for conical beam primaries. Both models have been evaluated in the present work. However, for the parameters considered, the effect of attenuation is negligible. The most recent model reported is by Mellen and Moffett<sup>9</sup>. This model is, in concept, closely related to Rolleigh's model<sup>7</sup>, but is evaluated numerically.

## 2.0 EXPERIMENT DESCRIPTIONS

The two experiments, the results of which are to be reported, both took place in fresh water. The experiments at TRANSDEC were conducted with the projector at a depth of 5.44 m in the tank. A block diagram of the experimental arrangement is shown in Figure 2-1(a). The projector, effectively a 20-inch diameter circular piston transducer, radiated the two primary frequencies simultaneously. The lower frequency was held constant at 42.50 kHz and had a measured source level of 226.2 dB re 1  $\mu$ Pa at 1 m. The higher primary frequency was varied from 43.58 kHz to 54.58 kHz and had a source level varying from 221.3 to 227.8 depending on the projector's transmitting response. The signals from the two oscillators were summed prior to power amplification. The receiving system consisted of an NUSC XU-1313 hydrophone followed by a lowpass filter and preamplifier and the standard TRANSDEC electronics. Output was channelled to a polar plotter, which produced beampatterns for all of the measurements.

The experimental configuration at Seneca Lake is shown in Figure 2-1(b). The projector, positioned behind a sonar dome, was suspended from the Transducer Calibration Platform (TCP) barge at a depth of approximately 76.0 m. The TCP electronics are similar to those at TRANSDEC and the preamp/filter box used was the same. Therefore, the only important difference in the receiving system was the use of an F-50 hydrophone. The signal generation used at Seneca Lake differed from that used at TRANSDEC. Rather than adding two primary frequencies, a modulator was used to produce single sideband ( $f_2$ ) plus carrier ( $f_1$ ). Other differences were the operation of the projector behind a dome, and a more powerful amplifier producing a primary source level outside the dome of 233.8 dB re 1  $\mu$ Pa at 1 m. For the measurements, the dome was positioned at the angle resulting in minimum beam distortion. Measurements at TRANSDEC indicated that the effect of the dome at this angle was to attenuate the primary source level and that the difference frequency source level seemed to behave as it should for the corresponding reduction in drive power. Therefore, the effect of the dome is believed to be negligible except to reduce the effective primary source level. Unlike the procedure followed in the TRANSDEC experiments, beampatterns were not drawn for each measurement. Rather, the beam was peaked up on the hydrophone and the axial source level was noted. The reason for this change of procedure was lack of time.

As mentioned in the introduction, during the TRANSDEC experiment the presence of intermodulation distortion in the receiving hydrophone was noted at short ranges and low frequencies by examining the shapes of the beampatterns. Figure 2-2 shows a rather extreme example of this. Figure 2-2(c) is the 1.5 kHz pattern at 24.0 m and is representative of the normal appearance of the parametric nearfield beampatterns showing no effect of distortion. Figure 2-2(b) is the corresponding pattern at 6.0 m and shows considerable elongation at the pattern tip caused by the very high primary frequency levels in the area of the major lobe. In figure 2-2(a), the 3.0 m pattern, the primary levels have become so high that intermodulation distortion dominates the parametrically generated signal even in the area of the first sidelobes.

The presence of the intermodulation distortion in the TRANSDEC data provided the motivation for the acquisition of nearfield data during the Seneca Lake tests. Unfortunately, very little was accomplished at Seneca Lake because there was so little time available after



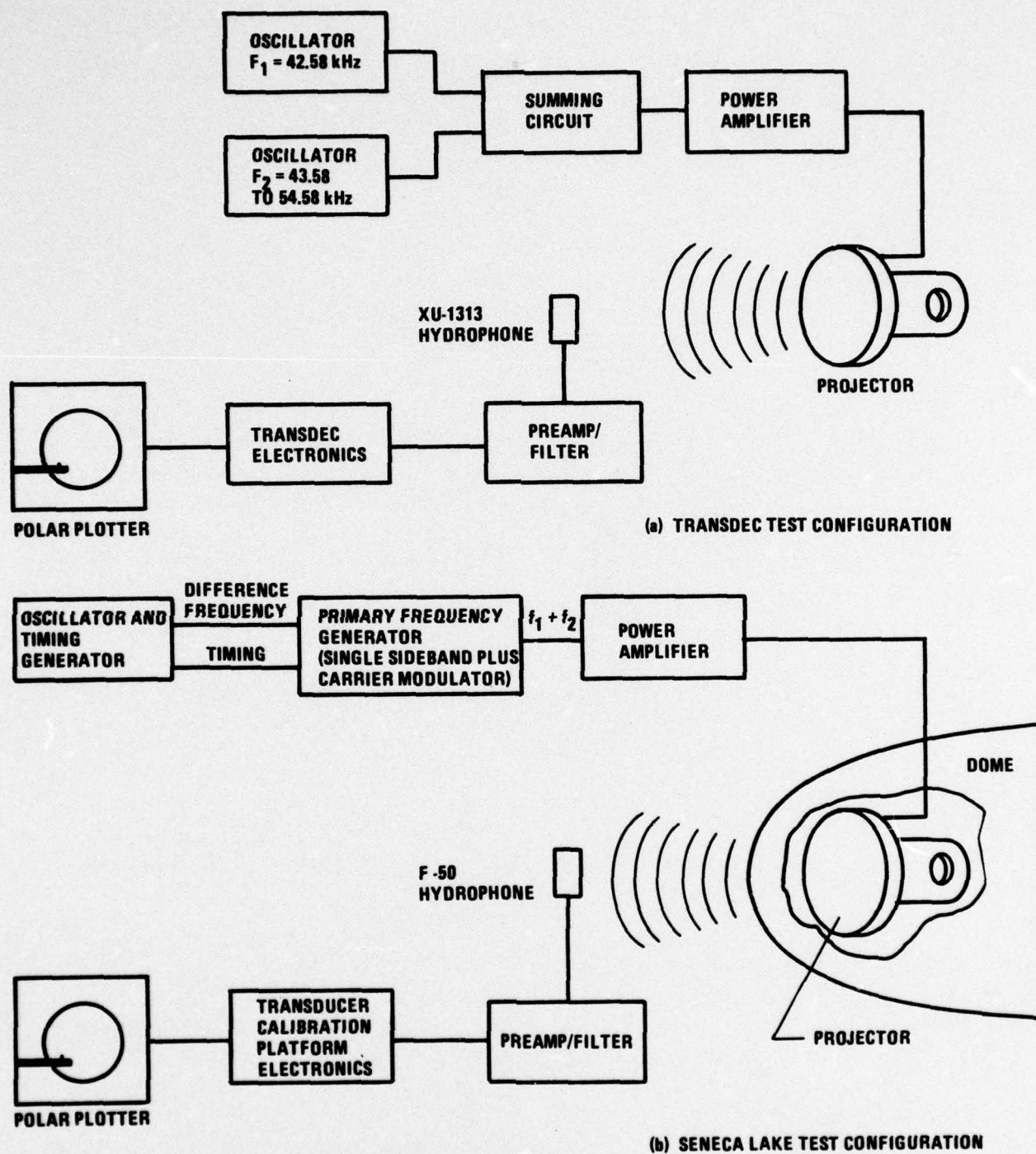
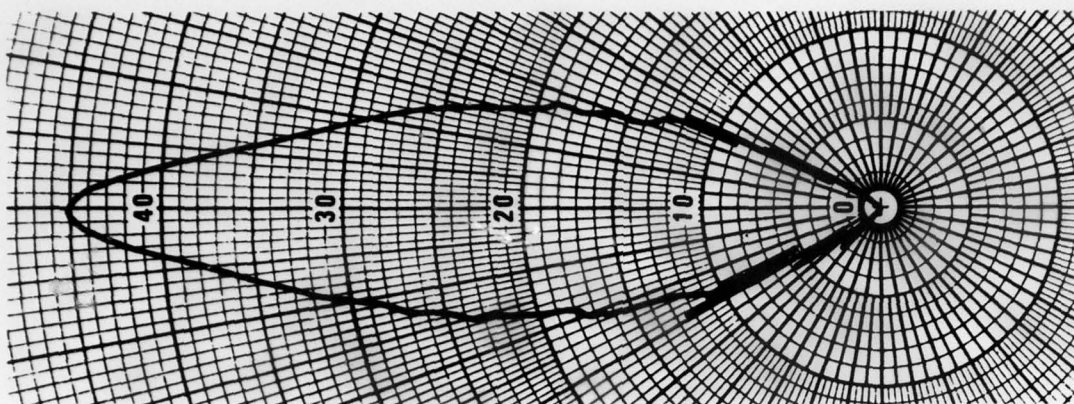
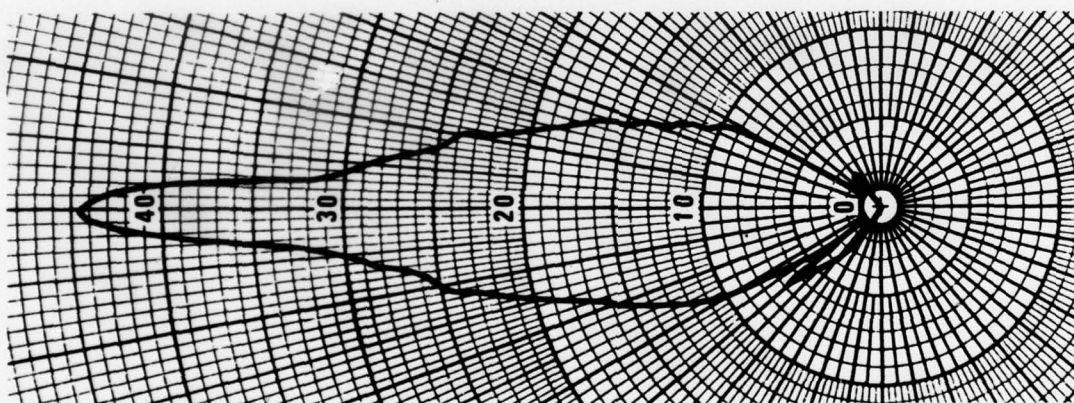


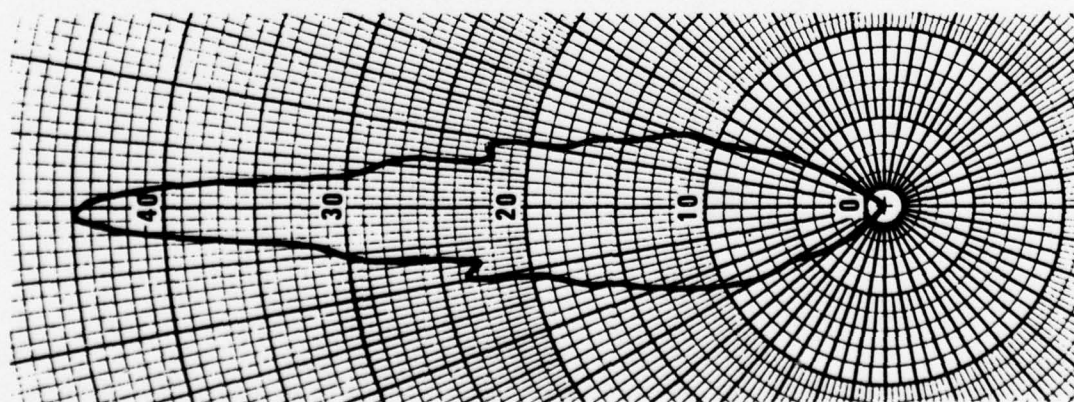
Figure 2-1. Test Configuration Functional Block Diagrams



(a) 1.5 kHz PATTERN AT 3.0 m



(b) 1.5 kHz PATTERN AT 6.0 m



(c) 1.5 kHz PATTERN AT 24.0 m

Figure 2-2. TRANSDEC Beam patterns Demonstrating Intermodulation Distortion



the farfield measurements were completed. There was one significant point demonstrated at Seneca Lake. That point was the power law dependence of the distortion. Figure 2-3 shows the 1.5 kHz data as measured at Seneca Lake. The data were taken at four primary source levels in 3.0 dB steps. The solid line is the theoretical curve according to the Muir-Willette<sup>1</sup> model evaluated for the highest source level. The great disparity between theory and experiment, particularly in the range dependence of the data, indicates that distortion is significant. The fact that the data for succeeding primary levels are almost exactly 6.0 dB apart shows that the dependence of the sum of signal and distortion on primary source level is quadratic. The parametric signal is known to be a quadratic function of primary level. Therefore, the fact that the range dependence does not change with primary source level indicates that the intermodulation distortion, is also a quadratic function of the primary frequency level. This demonstration that the intermodulation distortion goes as the square of the primary frequency pressure at the hydrophone makes it possible to attribute a 40.0 dB per decade range dependence to the intermodulation distortion in the farfield of the projector.

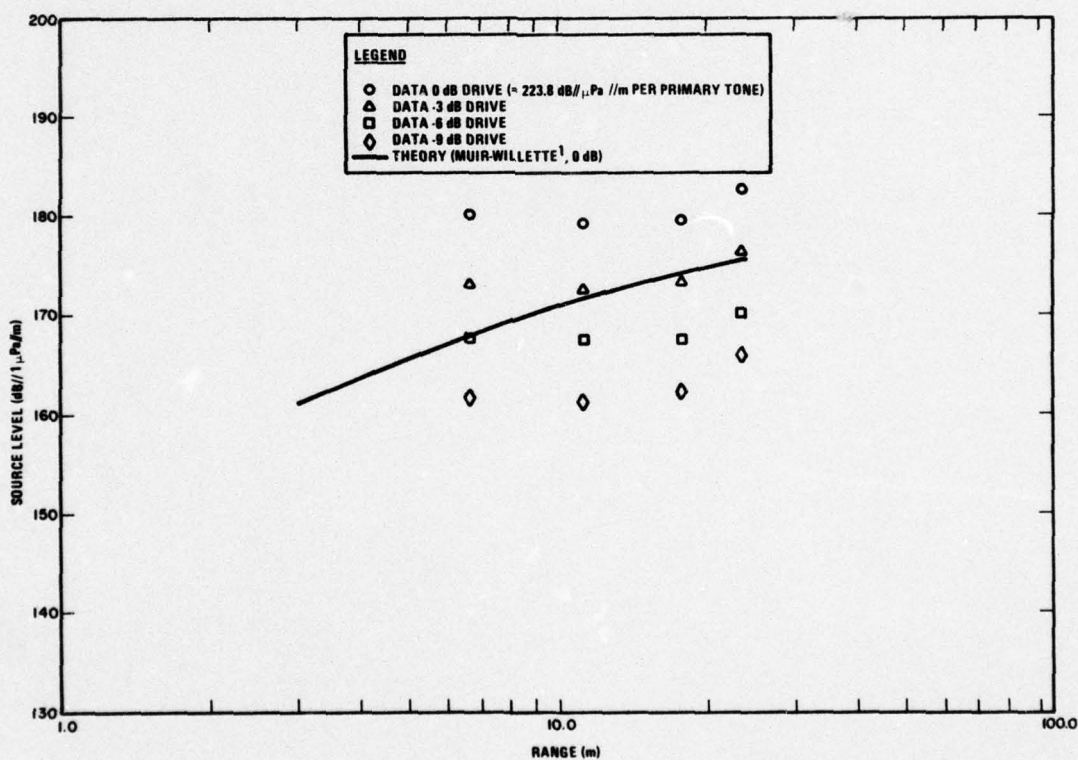


Figure 2-3. Secondary Frequency Source Level at 1.5 kHz as Measured for Four Drive Levels (Seneca Lake Experiment)

### 3.0 CORRECTION OF DATA

Because all of the data from the two experiments contain some amount of distortion, a method was sought to estimate the amount of error caused by the distortion and to perhaps correct the data. In order to do this, it was necessary to place some reliance on a theoretical model. However, this reliance was kept to a minimum by assuming that the theoretically derived levels for the two shortest range points had the correct ratio (difference in dB). Reliance on derived absolute levels was therefore avoided. The resulting corrected level for the shorter of the two ranges used is highly dependent on the theoretical ratio used. The other corrected values are quite insensitive to the assumed ratio, becoming less so as the range is increased.

The following assumptions were used in the correction procedure:

- 1) The measured pressure  $p_m$  is the sum of a signal pressure  $p_s$  and interference pressure  $p_i$ .
- 2) The interference pressure is proportional to the square of the primary pressure. The primary pressure is inversely proportional to range except in the nearfield. For nearfield points, the spherical wave correction given by Bobber<sup>10</sup> is used. With the nearfield correction expressed as a linear factor denoted by  $\delta$ , the interference pressure may be written

$$p_i = p_{io} \delta^2 / r^2$$

Note that  $\delta$  varies between 0 and 1, assuming the unity value in the farfield of the projector.

- 3) The signal levels at the two lowest ranges are proportional to the theoretical levels at those ranges, i.e., if  $p_{s1}$  and  $p_{s2}$  are the signal levels and  $p_{t1}$  and  $p_{t2}$  are the corresponding theoretical levels then

$$p_{s2} = \frac{p_{t2}}{p_{t1}} p_{s1}$$

The two lowest ranges are used because they contain the greatest proportion of interference and hence the least sensitivity to the actual signal level in estimating the interference pressure.

With the above assumptions, a system of equations may be written. At range 1 (eg. 3.0m) the measured pressure is written

$$p_{m1} = p_{s1} + p_{io} \delta_1^2 / r_1^2$$



At range 2 (eg. 6.0m), the measured pressure is written using assumption 3 above,

$$p_{m2} = p_{s1} \frac{p_{t2}}{p_{t1}} + p_{Io} \delta_2^2 / r_2^2.$$

For each frequency, the above equations can be solved for  $p_{Io}$ , which is then used to correct the data at all ranges. The only nearfield range point considered is the 3.0m point in the TRANSDEC experiment, for which the value of  $\delta_1$ , is 0.8224. In all other cases,  $\delta_1 = \delta_2 = 0$ . The Lockwood<sup>5</sup> model was used to provide the theoretical ratio.

#### 4.0 EXPERIMENTAL RESULTS

The experimental data obtained at TRANSDEC are plotted in Figures 4-1 through 4-10. In each figure the measured data are shown as solid circles. The solid line represents theory calculated using Lockwood's model<sup>5</sup> and the dashed line represents theory calculated from the Muir-Willette<sup>1</sup> model. The crosses represent corrected data, calculated assuming that the Lockwood theory has the correct short range slope.

The two theories are shown because they demonstrate the contrast between the results of different types of approximations. Other theories are compared in the next section. At the larger ranges it would be initially expected that the Muir-Willette model would be more correct than the Lockwood model because of the explicit inclusion of the primary frequency beam pattern. However, for reasons discussed in the next section, the Muir-Willette results may be as much as 1.0 dB conservative. The Lockwood model is expected to be more correct at ranges below 6.0 m because of the inclusion of a planewave nearfield.

The source levels used in the TRANSDEC experiments were easily low enough to make finite-amplitude attenuation negligible. Under such conditions, the secondary pressure increases as the square of the primary pressure and for every 1.0 dB of increase in the mean primary source level the secondary source level increases 2.0 dB. For convenience the theoretical data were all calculated using a mean primary frequency source level of 227.8 dB// $\mu\text{Pa}/\text{m}$ , and the measured data shown in Figures 4-1 through 4-10 have been scaled up by twice the source level difference. The amounts by which the levels at each frequency have been increased are shown in Table 4-1. In a few cases more than one data value was obtained. These generally agreed within about 1.0 dB and are shown here as average values.

There is a considerable variability in which theory best fits the data. When there is a theoretical discrepancy of 2.0 dB it is difficult to resolve even by distortion free measurements because of the quadratic dependence on the primary source level. The test facilities are considered to have accuracies of about  $\pm 1.0$  dB and a 1.0 dB error in estimating the primary frequency source level leads to a 2.0 dB error in the secondary level. In any case, Figure 4-1 shows corrected data that are very close to the dashed Muir-Willette<sup>1</sup> curve, the solid Lockwood<sup>5</sup> curve being higher. In Figure 4-2, the 12 m data point is not really consistent but otherwise the Muir-Willette theory is favored. In Figure 4-3, the 3.0 m point was discarded because it led to unreasonable corrected levels. The remaining points tend to agree with the dashed line. In Figure 4-4, the solid line is favored. The data in Figure 4-5 also favor the Lockwood curve. Figure 4-6 does not really favor either curve. It appears that in this case, the correction procedure resulted in too high a distortion level. In Figures 4-7 through 4-10 the trend is toward data that support both theories equally well.

The data obtained at Seneca Lake are shown in Figures 4-11 through 4-13. Here, data were obtained at only three frequencies. The primary source level was a constant 233.8 dB// $\mu\text{P}/\text{m}$  per tone, still too low for significant finite-amplitude effects at these ranges. The minimum range for these data was 6.74 m, limited by the test configuration. There is a general tendency for these data to be high. They give a reasonable fit to the solid curves, but are significantly higher than the dashed curves.



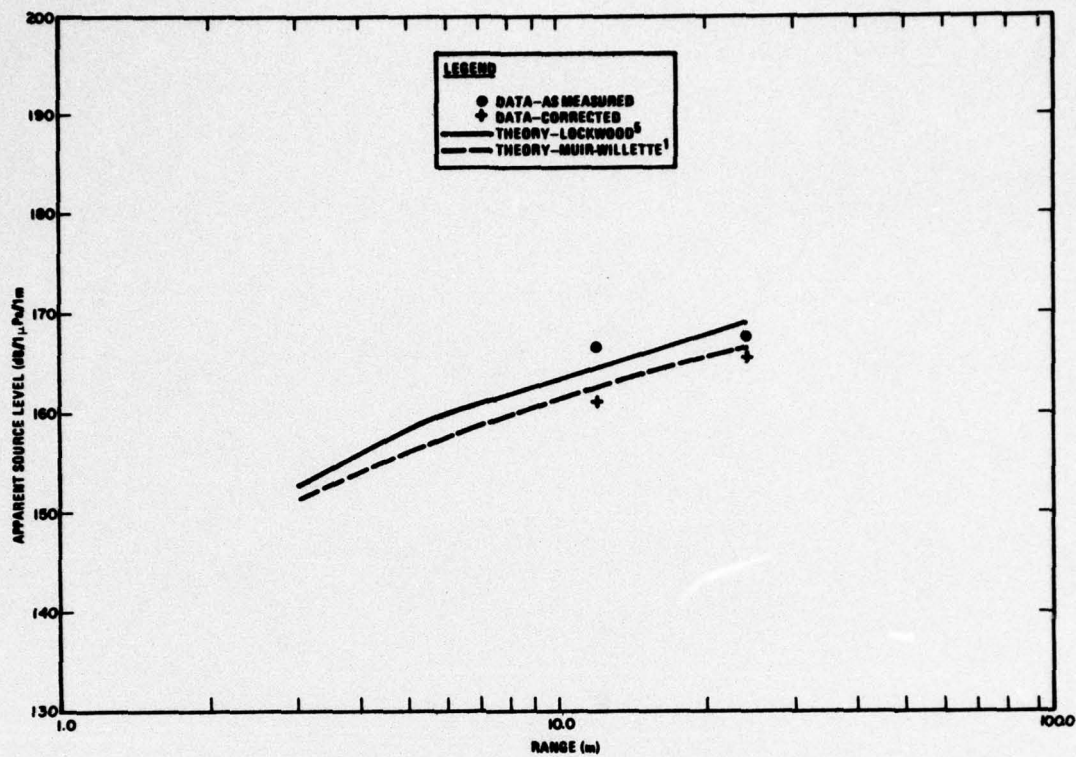


Figure 4-1. TRANSDEC Data at 1.0 kHz Difference Frequency

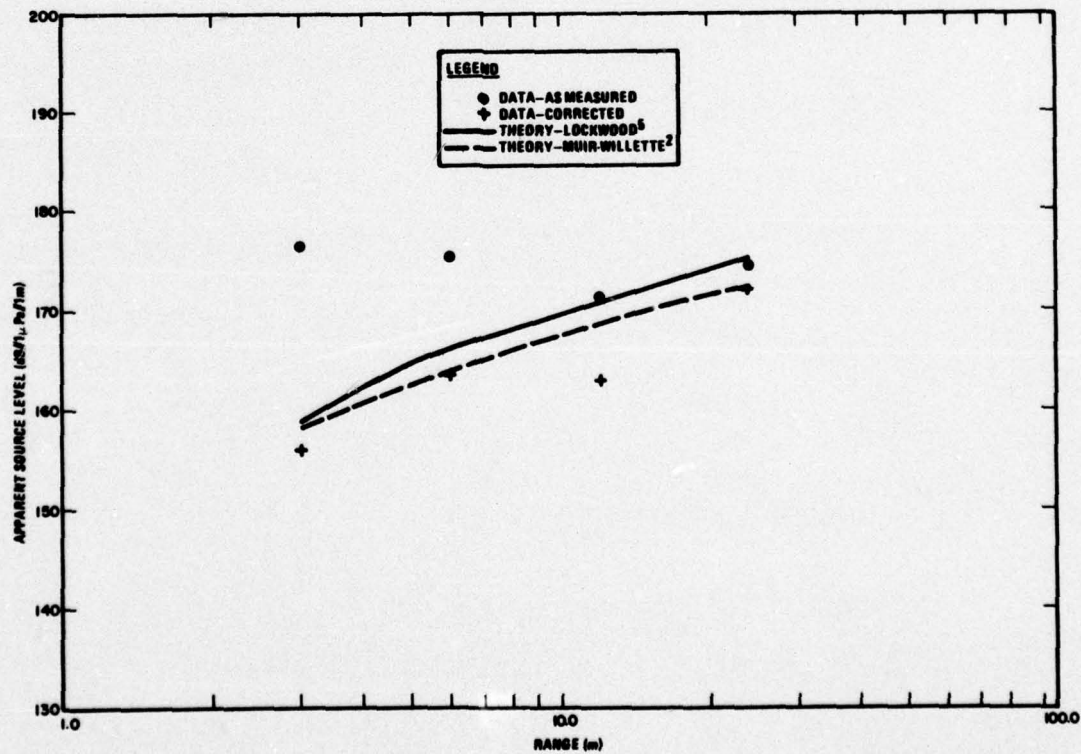


Figure 4-2. TRANSDEC Data at 1.5 kHz Difference Frequency

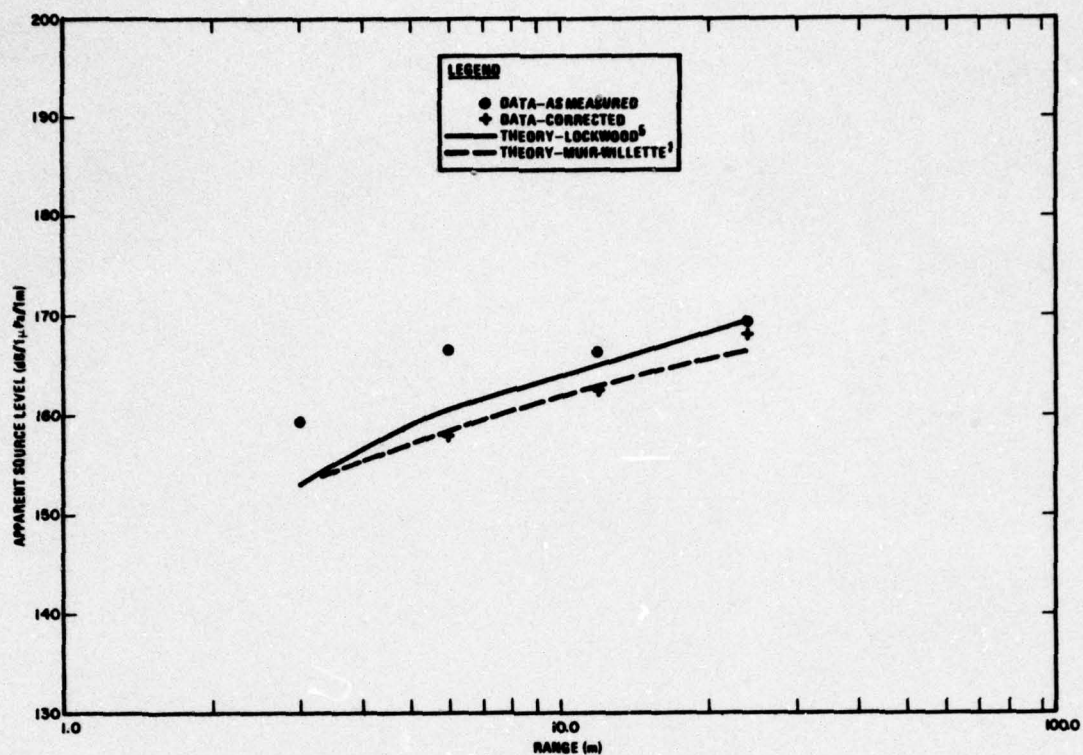


Figure 4-3. TRANSDEC Data at 2.0 kHz Difference Frequency

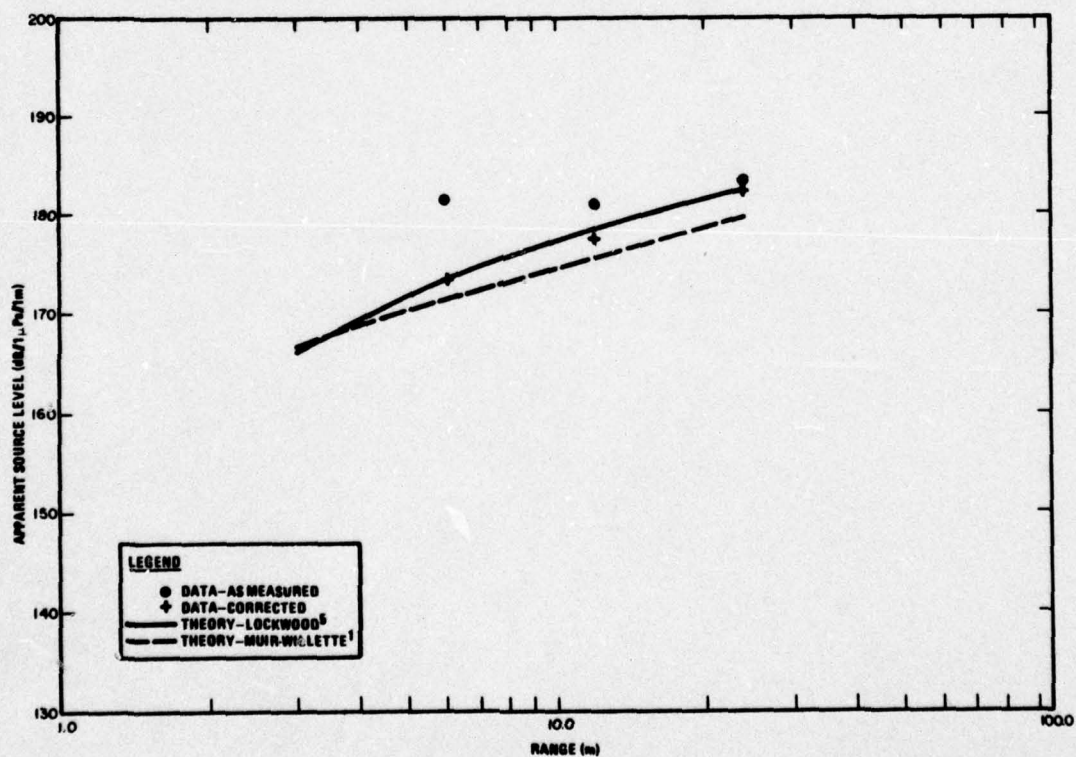


Figure 4-4. TRANSDEC Data at 2.5 kHz Difference Frequency

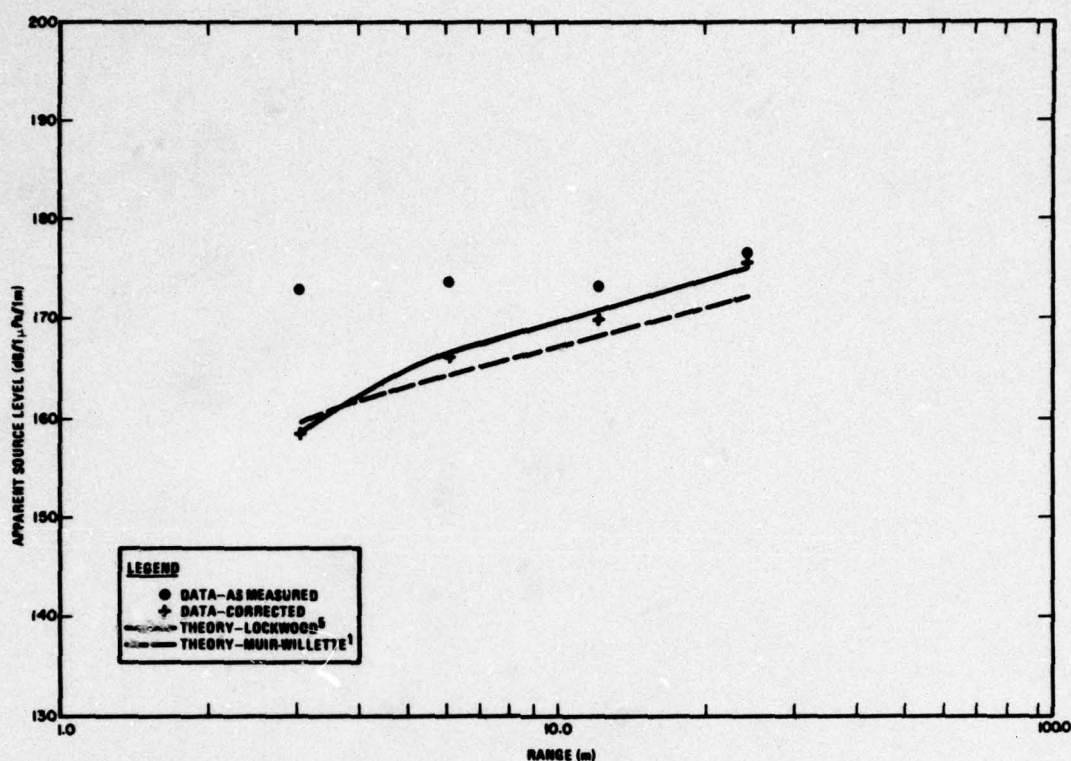


Figure 4-5. TRANSDEC Data at 3.0 kHz Difference Frequency

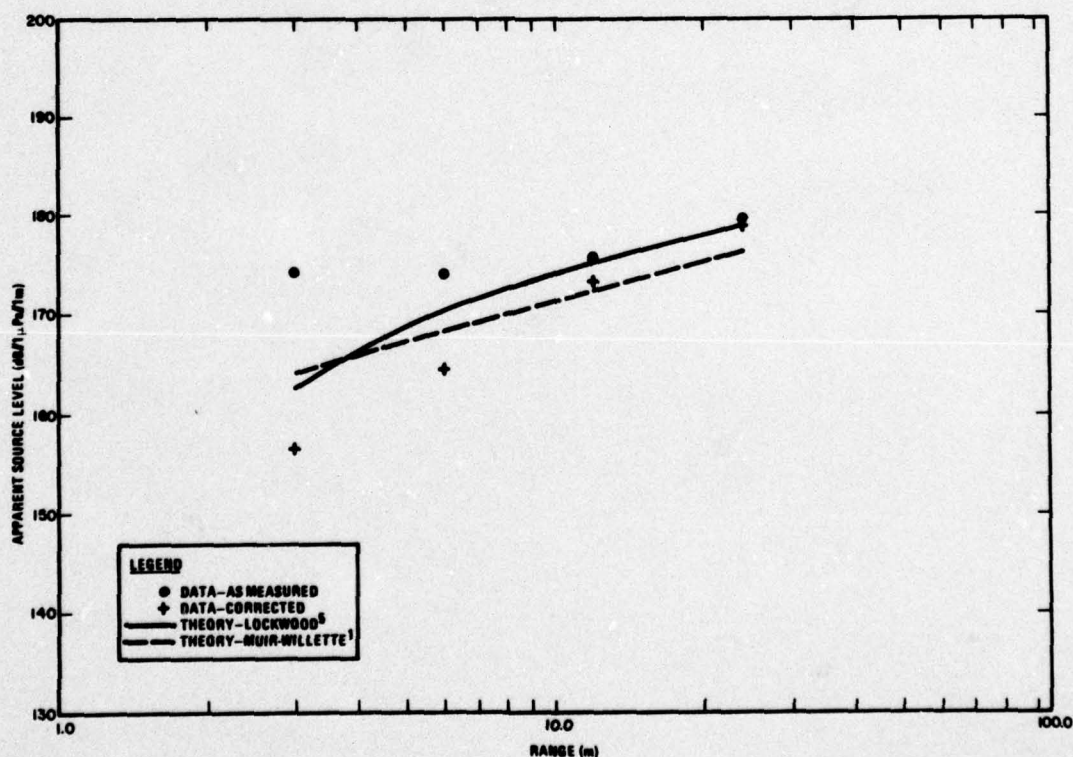


Figure 4-6. TRANSDEC Data at 4.0 kHz Difference Frequency



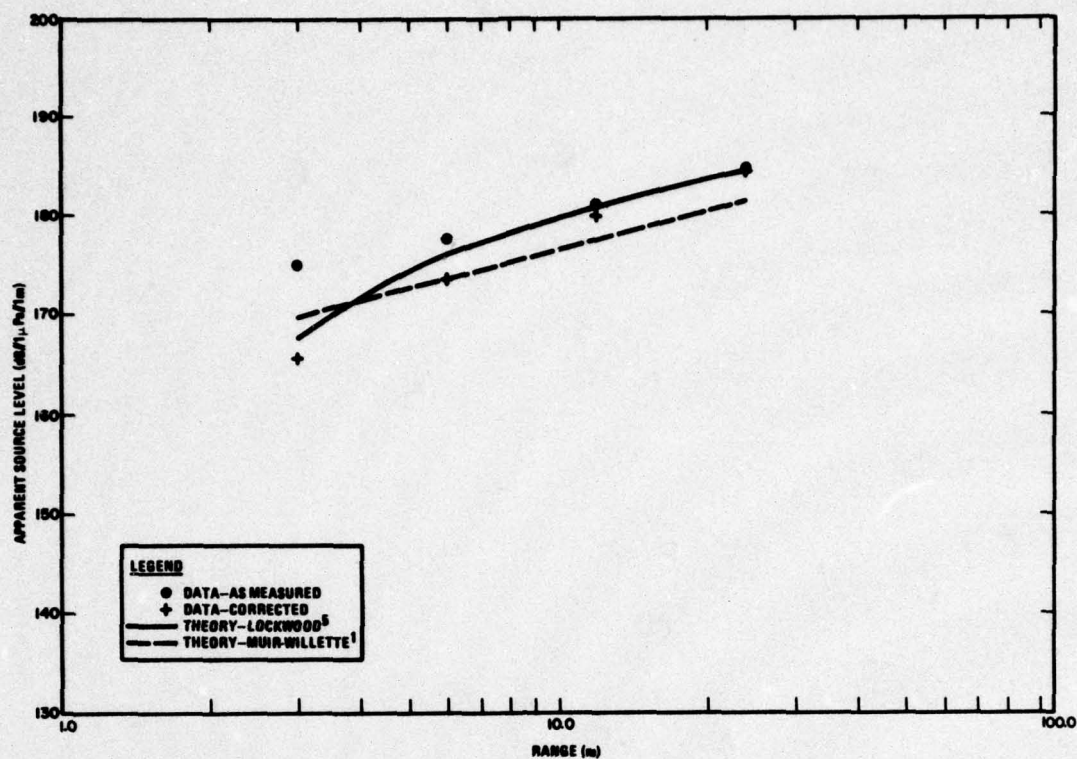


Figure 4-7. TRANSDEC Data at 6.0 kHz Difference Frequency

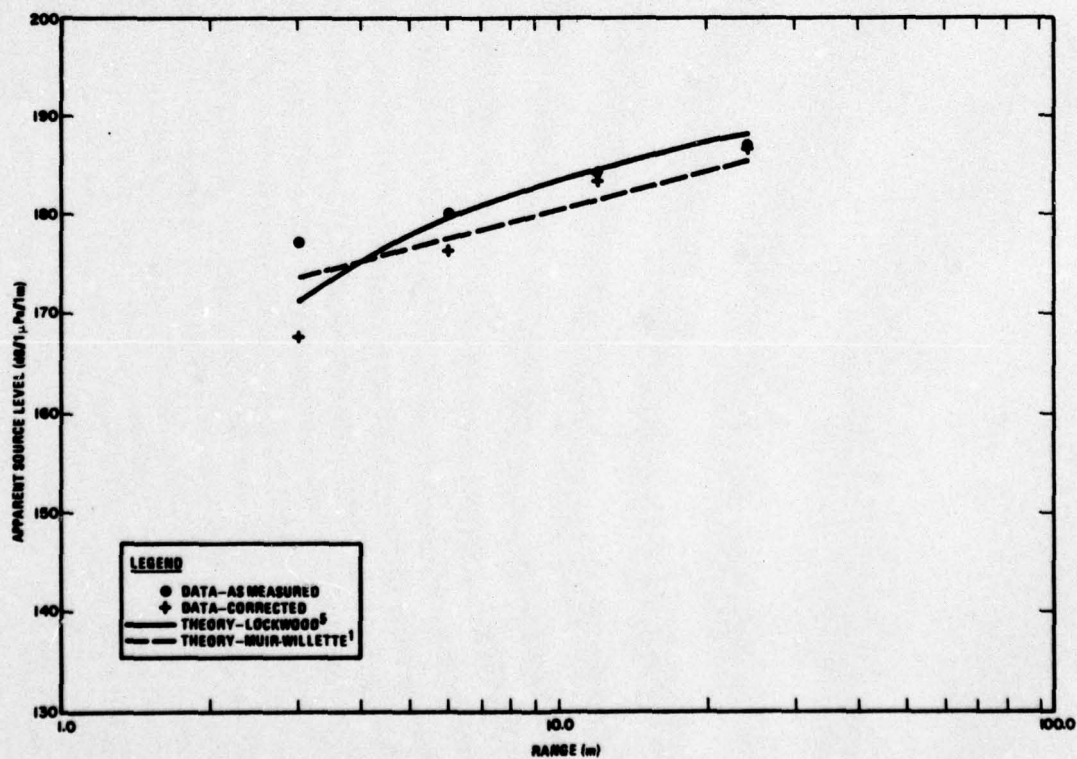


Figure 4-8. TRANSDEC Data at 8.0 kHz Difference Frequency



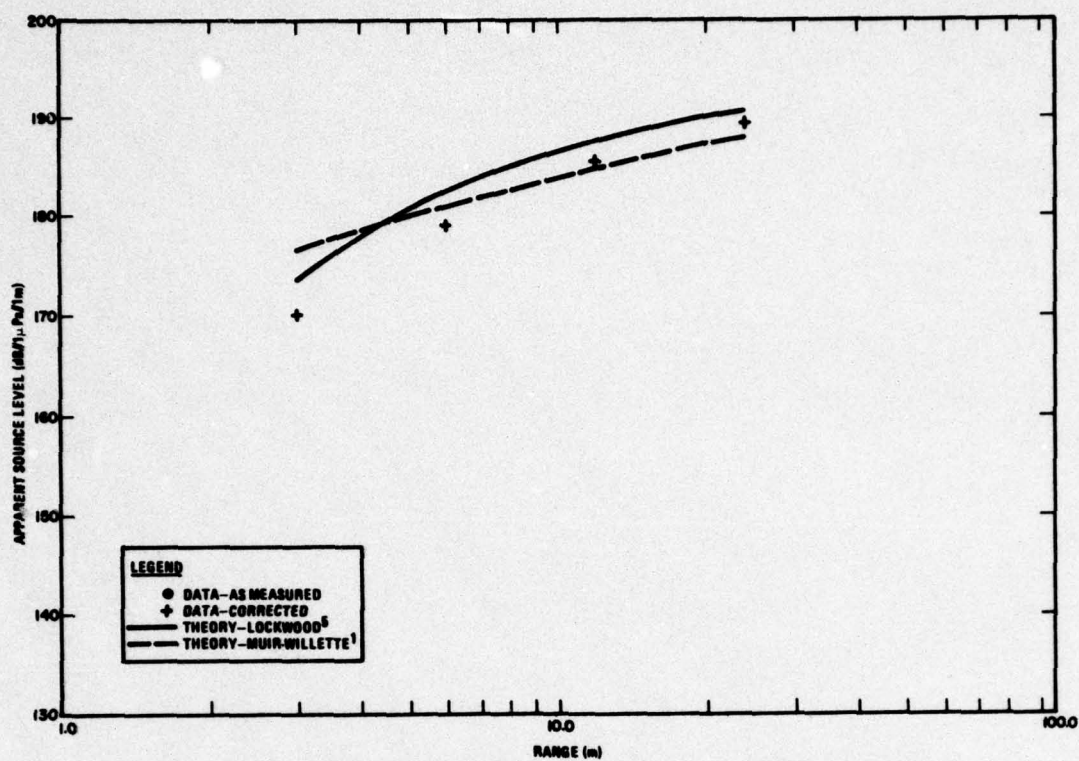


Figure 4-9. TRANSDEC Data at 10.0 kHz Difference Frequency

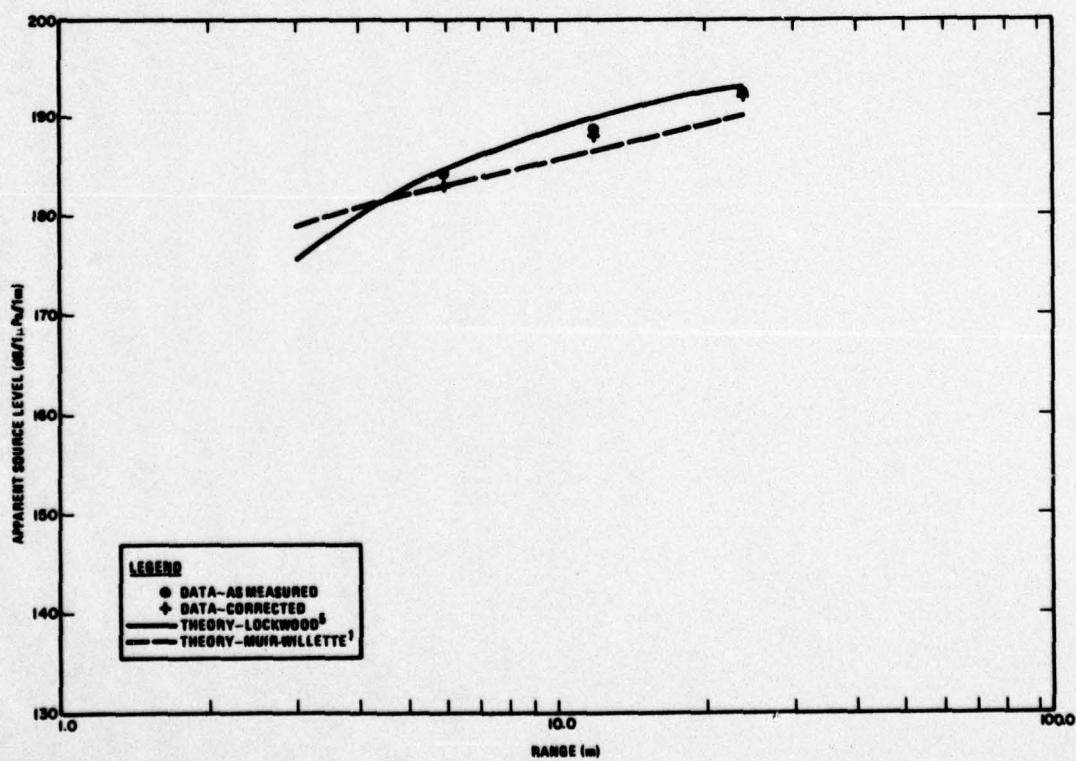
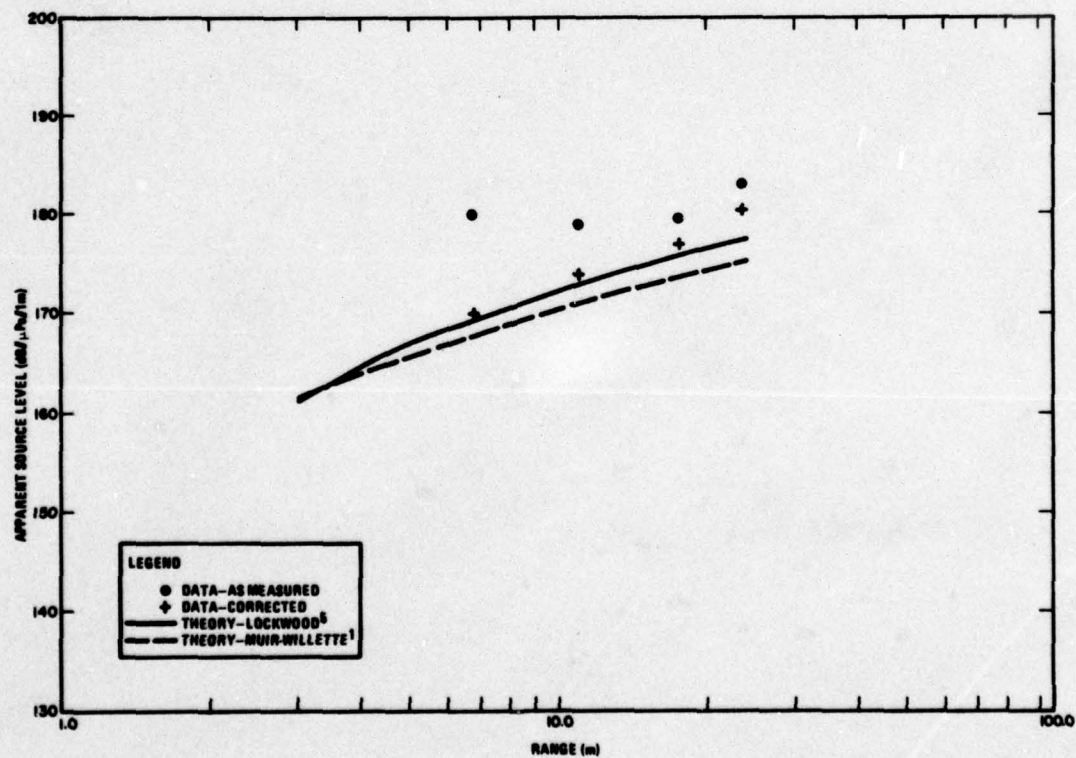


Figure 4-10. TRANSDEC Data at 12.0 kHz Difference Frequency

**Table 4-1. Measured Data Increases to Compensate for Assumed Constant Mean Source Level**

Difference Frequency	Correction (dB)
1.0	2.2
1.5	1.8
2.0	1.6
2.5	1.6
3.0	1.9
4.0	1.9
6.0	4.6
8.0	6.0
10.0	7.5
12.0	8.1



**Figure 4-11. Seneca Lake Data at 1.5 kHz Difference Frequency**



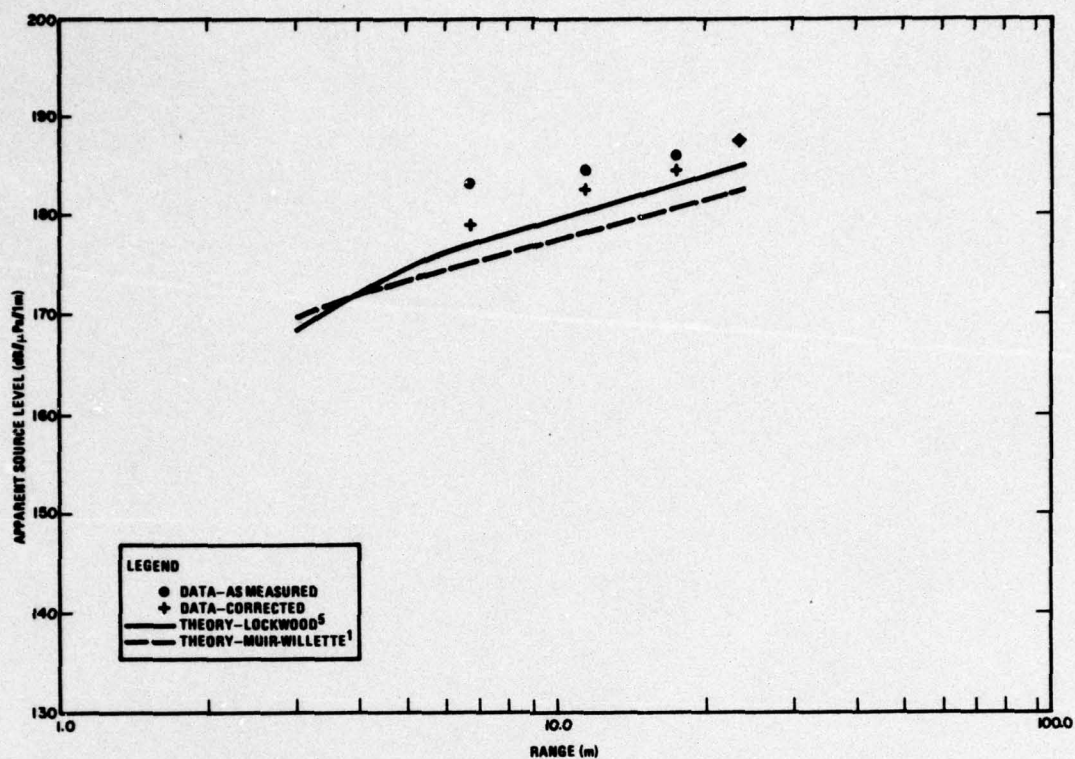


Figure 4-12. Seneca Lake Data at 2.5 kHz Difference Frequency

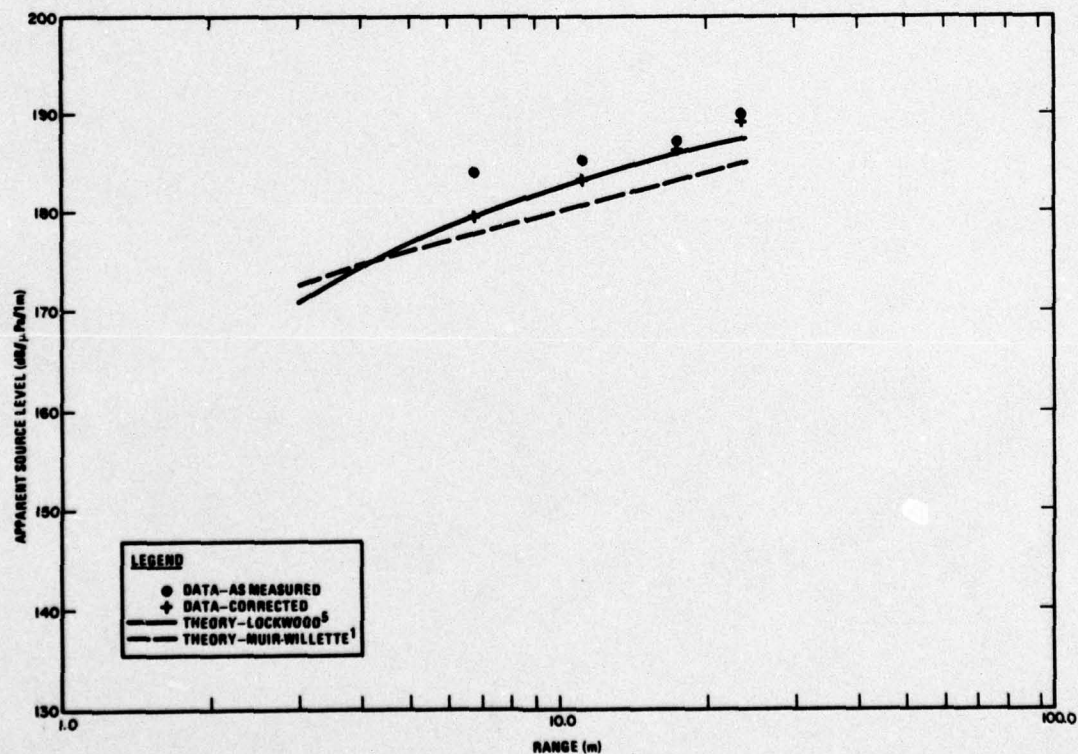


Figure 4-13. Seneca Lake Data at 3.0 kHz Difference Frequency

## 5.0 COMPARISON OF THEORETICAL RESULTS

A convenient way of looking at the parametric array nearfield has the interaction volume divided into apertures formed by slicing the primary beam perpendicular to its acoustic axis. Each such aperture radiates secondary signals with a farfield level that depends on the amplitude and phase distribution of the source strength density in the aperture and on the distance from the aperture to the measurement point. Each aperture also has a nearfield. The amplitude and phase at a measurement point is the sum of the signals from all of the apertures from the projector out to the measurement point.

The accuracy of any nearfield model, assuming that loss mechanisms may be neglected, depends on the accuracy with which the primary field is modeled and on the accuracy with which the contributions of all the virtual sources are summed at the measurement point. Most of the nearfield models that have been proposed treat the primary beam as a spherically spreading wave retaining the assumed farfield characteristics all the way back to the source. The exceptions are the strictly cylindrical-beam models such as those of Berklay<sup>3</sup> and of Mellen<sup>8</sup>, and Lockwood's model<sup>5</sup>, which combines a planewave nearfield and a spherically spreading farfield. The conical beam models are not applicable to measurement points in the primary beam's nearfield. Another issue concerning the description of the primary beam is the assumed beampattern. In the models of Bartram<sup>4</sup>, Mellen<sup>8</sup> and Lockwood<sup>5</sup>, the far-field beam is assumed to be conical, with equal amplitude over a spherical cap, and with energy equal to the total radiated energy. A description that is, in principle, more precise incorporates the theoretical beampattern of the projector. The Muir-Willette<sup>1</sup>, Rolfeigh<sup>7</sup> and the new Mellen-Moffett<sup>9</sup> nearfield models are examples of this type of treatment. It turns out that there is generally a discrepancy of about 2.0 dB for cases considered in the present work between models incorporating the primary beampattern and those not. This is because the major lobe of the circular piston pattern accounts for only about 80% of the radiated energy. While the assumption that 100% of the primary frequency energy contributes to the secondary source strength clearly represents an upper bound, the models that incorporate the beampattern tend to be conservative for two reasons. First, they all assume that the primary beampattern applies all the way back to the source. It seems reasonable to expect 100% of the primary frequency energy to contribute in the projector nearfield because the sidelobe energy is still in the column. The second reason is that it is usual to assume that negligible signal comes from outside the major lobe. In the Muir-Willette model<sup>1</sup>, for example, the integration over angle is only carried out to the first null of the primary pattern. Yet, in nearfield cases, energy from the sidelobes may be significant. A preliminary test of the Muir-Willette model in which the angle included in the integration was quadrupled showed an increase of about 0.3 dB for cases of present interest. From the two reasons combined, the models may well be low by as much as 1.0 dB at 24.0 m and even more at shorter ranges that are still in the projector farfield.

There are two significant issues related to the accuracy with which the contributions of all of the virtual sources are summed at the measurement point. The most basic consideration is that the variation of the range from the measurement point to each virtual aperture be



accounted for. All nearfield models do this. The other issue is the handling of the apertures for which the measurement point is in the nearfield. Because of their proximity to the measurement point, phase varies rapidly over these apertures, and care should be taken to see that they are properly described. The accuracy of the various models in this regard and the quantitative effect of errors are difficult to assess.

Six of the theories discussed above have been evaluated for the conditions of the Seneca Lake experiment. The results for frequencies of 1.5, 3.0 and 10.0 kHz are shown in Figures 5-1 through 5-3. The theories represented by lines are those of Bartram<sup>4</sup>, Rolleigh, Lockwood<sup>5</sup>, Muir and Willette<sup>1</sup>, and Mellen<sup>8</sup> (cylindrical and conical versions). Because of the assumptions of a conical primary beam, none of the theories shown are expected to be valid within 6.0 m except for the Mellen<sup>8</sup> cylindrical model and the Lockwood<sup>5</sup> model. These two models are in reasonable agreement between 3.0 and 6.0 m, although the Lockwood model appears to be relatively low at the 10 kHz frequency. If one discounts the Mellen cylindrical model beyond 6.0 m, then all of the theoretical results fall within about 3.0 dB at 1.5 kHz, 3.5 dB at 3.0 kHz and 4.5 dB at 10.0 kHz. The increase in spread appears to be attributable solely to a drop in the Muir-Willette<sup>1</sup> curve relative to the others. However, on close inspection, it is observed that the Muir-Willette<sup>1</sup> and Lockwood<sup>5</sup> theories appear to retain a constant ratio as frequency is varied. Also, the Bartram<sup>4</sup> and Rolleigh<sup>7</sup> theories tend to keep the same ratio but to change relative to the Muir-Willette and Lockwood theories. The Mellen<sup>8</sup> (conical) curve does not seem to consistently track either of the pairs of theoretical curves mentioned above.

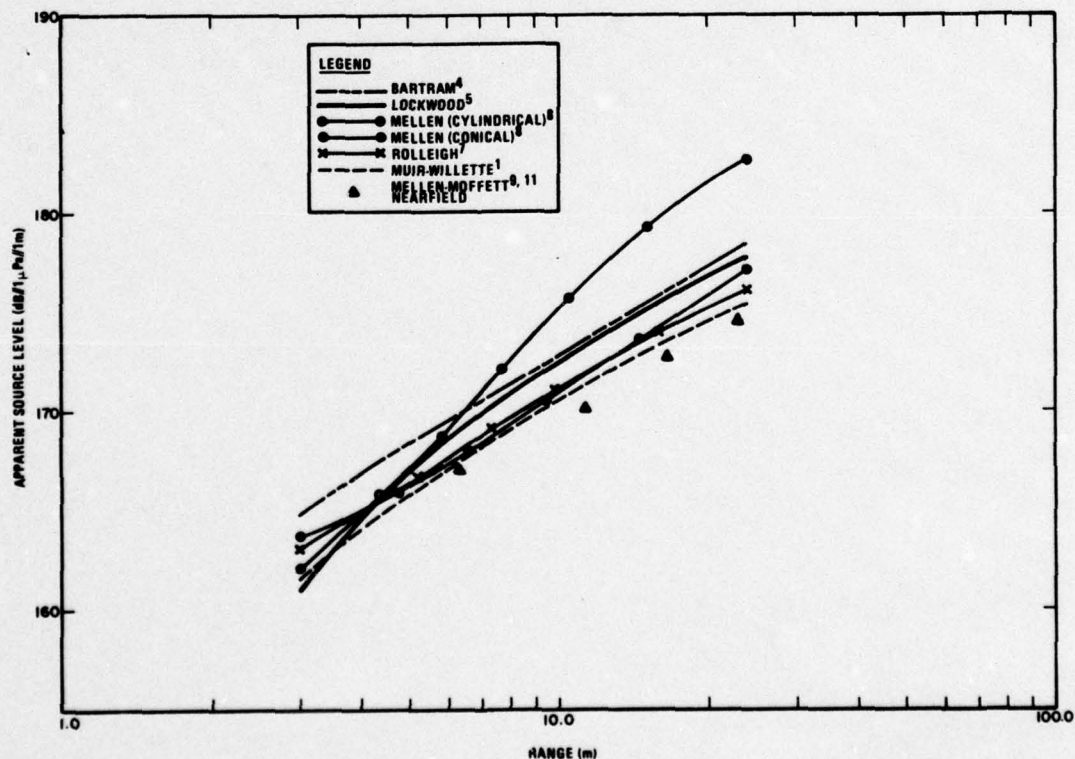


Figure 5-1. Comparison of Theoretical Data for 1.5 kHz Difference Frequency (Conditions of Seneca Lake Experiment Assumed)

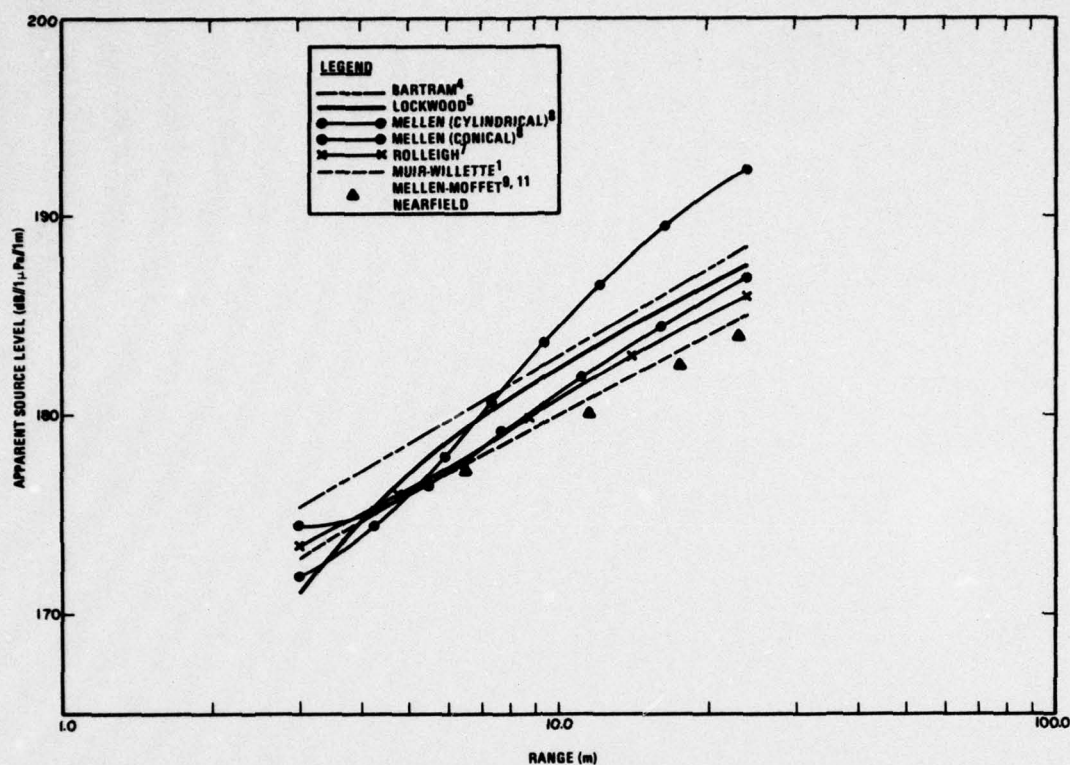


Figure 5-2. Comparison of Theoretical Data for 3.0 kHz Difference Frequency (Conditions of Seneca Lake Experiment Assumed)

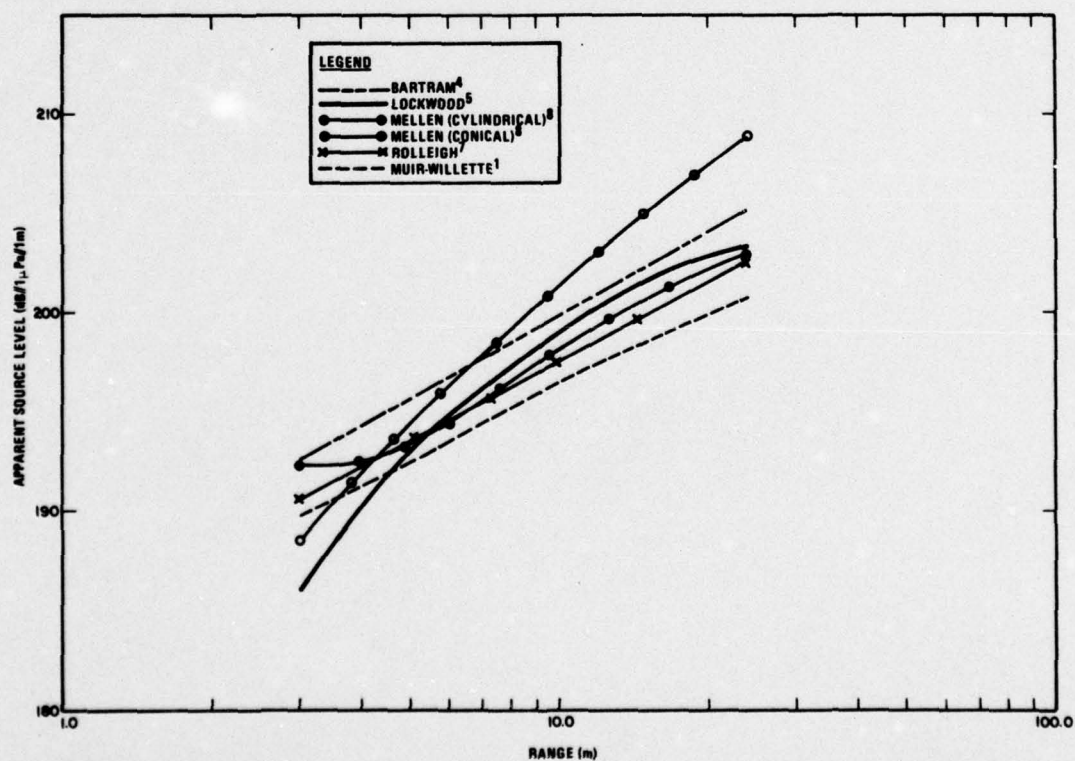


Figure 5-3. Comparison of Theoretical Data for 10.0 kHz Difference Frequency (Conditions of Seneca Lake Experiment Assumed)



The reason for this shift with frequency of two theories relative to two others is not fully understood, but is believed to be related to the method of handling the apertures that are in the nearfield relative to the observation point. The shift at short ranges of the Mellen (cylindrical) theory relative to the Lockwood theory may also be related to the handling of nearfield apertures.

The offset between the Bartram<sup>4</sup> and Rolfeigh<sup>7</sup> theories and between the Lockwood<sup>5</sup> and Muir-Willette<sup>1</sup> theories at ranges greater than the projector's nearfield distance is believed to be caused by the explicit account of the primary frequency beampattern in the Rolfeigh and Muir-Willette models. In each case, the offset is about 2.0 dB. It is interesting to note that 2.0 dB is the approximate ratio of the total radiated energy to the energy in the main lobe for the projector considered. The Bartram and Lockwood models assume that all of the radiated energy goes into the interaction, whereas the models that incorporate a beampattern include little that is not in the major lobe. A 2.0 dB discrepancy is therefore consistent with this fact.

Although the inclusion of the beampattern is, in principle, more accurate than the simpler model, in practice, the results tend to be conservative. This is largely because of the use of the approximation that the primary beam is conical all the way to the origin. In the primary nearfield, it seems reasonable to expect all of the energy to contribute to the secondary signal, not just the 80% in the major lobe. In fact, it might be argued that all energy within the first Fresnel zone relative to the observation point should contribute. A further effect of using the theoretical beampattern that may lead to erroneous results is the non-ideal nature of the primary frequency beampattern. High sidelobe levels may increase the amount of energy contributing to the axial secondary signal. For conditions of the present experiments, the explicit inclusion of the primary frequency beampattern combined with the conical beam assumption is estimated to lead to results that are too low by a minimum of 0.5 dB at 24.0 m. An error of as much as 1.0 dB is not unlikely. Therefore, it appears that if two models were precisely correct in all respects except the handling of the primary beampattern, then the version with the theoretical beampattern included should provide a lower bound, the model assuming all radiated energy to occupy a constant amplitude cone should provide an upper bound, and the "true" value should lie in the middle.

In summary, all models considered are within 3.0 dB in their regions of applicability at 1.5 kHz. The spread among the results increase as frequency is increased, with the Bartram and Rolfeigh data maintaining an approximately constant ratio and the Lockwood and Muir-Willette data maintaining an approximately constant ratio. In each case, the constant ratio is approximately 2.0 dB and can be attributed to the handling of the primary beampattern. The disparity between the Bartram and Rolfeigh models on one hand and the Lockwood and Muir-Willette models on the other is unexplained, but is believed related to the handling of geometry close to the measurement point.

The data represented by triangular points on Figures 5-1 and 5-2 have been left for discussion at the end of the section because they were not evaluated by the present author and are not available at the entire span of ranges and frequencies considered. These data were supplied by Moffett<sup>11</sup> using parameters supplied by the author for the conditions of the Seneca Lake experiment. These data from the new Mellen-Moffett<sup>9</sup> nearfield model agree quite well with the Muir-Willette<sup>1</sup> results, but tend to be lower, in some cases by as much as 1.0 dB.

## 6.0 CONCLUSIONS

Results from two parametric nearfield experiments have been reported. The data, known to contain substantial receiving hydrophone intermodulation distortion, have been corrected by deducing the level of the distortion and coherently subtracting the distortion pressure from the measured data. The data obtained at TRANSDEC at ten frequencies support both the Lockwood<sup>5</sup> and the Muir-Willette<sup>1</sup> theories quite well. Note that the latter is not considered valid at ranges less than 6.0 m; so any disagreement in this region is disregarded. Because the data seem to support both theories equally well, they especially support the contention that the two theories are, respectively, upper and lower bounds. Comparison with other theories considered may be effected indirectly by referring to Figures 5-1 through 5-3. Although the figures were prepared for the conditions of the Seneca Lake experiment, the comparison of relative levels for a given frequency is equally applicable to the TRANSDEC experiment conditions.

When the theories are compared in light of the TRANSDEC data, it appears that the Bartram<sup>4</sup> theory has a tendency to be high. The Rolfeigh<sup>7</sup> and Mellen<sup>8</sup> (conical) theories, in the primary farfield where they are valid, tend to lie between the Lockwood<sup>5</sup> and Muir-Willette<sup>1</sup> curves and so agree well with the experimental data. The fact that these models tend to shift with frequency relative to the Lockwood and Muir-Willette curves is somewhat disturbing.

The Seneca Lake data tend to be somewhat high relative to the Muir-Willette and Lockwood curves, giving a reasonable fit only to the latter. However, the conditions under which these data were obtained are such that little confidence can be associated with them.

A test of several nearfield theories has been made. Because of the condition of the experimental data, the test is not particularly discriminating. Also, there is not a great deal of spread among the theories considered. Within their regions of validity, the theories of Rolfeigh<sup>7</sup>, Mellen<sup>8</sup>, Muir and Willette<sup>1</sup> and Lockwood<sup>5</sup> all give good agreement with experiment. Of these, the last is the only one that is uniformly valid at points in both the nearfield and farfield of the projector.

In conclusion, it is of interest to compare the difficulty of applying the various models considered. Table 6-1 gives for each model the degree of difficulty on a scale of 1 (easy) to 10 and the minimum equipment requirement for evaluation.



*Table 6-1. Degree of Difficulty and Equipment Required for Each Model*

Model	Difficulty	Equipment Required
Bartram <sup>4</sup>	1	Slide Rule
Mellen <sup>8</sup>	2	Slide Rule
Lockwood <sup>5</sup>	3	Programmable Calculator
Muir-Willette <sup>1</sup>	10	Large Computer
Rolleigh <sup>7</sup>	1	Slide Rule
Mellen-Moffett Nearfield <sup>9</sup>	10	Large Computer

7.0 LIST OF REFERENCES

1. T.G. Muir and J.G. Willette, "Parametric Acoustic Transmitting Arrays," J. Acous. Soc. Am. 52, 1481 (1972).
2. T.G. Muir, L.L. Mellenbruch and J.C. Lockwood, "Reflection of Finite-Amplitude Waves in a Parametric Array," J. Acous, Soc. Am. publication pending.
3. H.O. Berkday, "Nearfield Effects in Parametric End-Fire Arrays," J. Sound Vib. 20, 135 - 143 (1972).
4. J.F. Bartram and R.P. Fugitt, "Nearfield Effects in a Parametric Transmitting Array," 87th Meeting of the Acoustical Society of America, New York, April 1974.
5. J.C. Lockwood and D.P. Smith, "Investigation of the Increase in Parametric Efficiency Due to Bubbles, " Final Report under Contract N00024-74-C-1151, AMETEK, Straza Div., El Cajon, CA, August 1974.
6. R.H. Mellen and M.B. Moffett, "A Model for Parametric Sonar Radiator Design," Naval Underwater Systems Center, Technical Memorandum No. PA4-229-71 (Sept. 1971).
7. R.L. Rolleigh, "Difference Frequency Pressure Within the Interaction Region of a Parametric Array," J. Acous. Soc. Am. 58, 964 -971 (1975).
8. R.H. Mellen, "A Nearfield Model of the Parametric Radiator," Naval Underwater Systems Center, Technical Memorandum No. PA4-230.75, December 1975.
9. R.H. Mellen and M.B. Moffett, "Numerical Method for Calculating the Nearfield of a Parametric Acoustic Source," J. Acous. Soc. Am. 61, S83 (A) (1977).
10. R.J. Bobber, Underwater Electroacoustic Measurements (U.S. Government Printing Office, Washington, D.C. 1970).
11. M.B. Moffett, Private Communication, June 1977.



## APPENDIX A

In this appendix is supplied for reference a FORTRAN listing of the main program and required subprograms used to evaluate the Muir-Willette model. The original model is described in Reference 1. Modifications made by the author are noted in the comments at the beginning of the listing.

77/07/08. 10.52.40

FTN 4.6+428

73/74 OPT=1

```

1      PROGRAM WILLET(INPUT,OUTPUT)
      THIS PROGRAM COMPUTES THE AXIAL SOURCE LEVEL OF A PARAMETRIC
      ARRAY BY THE VOLUME INTEGRATION METHOD. THE PROGRAM WAS
      ORIGINALLY WRITTEN BY J. G. WILLETTE AT APPLIED RESEARCH
      LABORATORIES, THE UNIVERSITY OF TEXAS AT AUSTIN. SUBSTANTIAL
      MODIFICATIONS WERE SUBSEQUENTLY MADE BY J. C. LOCKWOOD.
      THESE MODIFICATIONS INCLUDE 1) THE INCLUSION OF A FINITE
      AMPLITUDE TAPER FUNCTION, 2) REVISION OF THE INPUT PARAMETERS
      TO SI UNITS, AND 3) APPLYING A SINH STRETCHING TO THE RANGE
      VARIABLE TO REDUCE THE NUMBER OF INTEGRATION STEPS REQUIRED
      FOR CONVERGENCE.

```

```

      PROGRAM INPUT REQUIRES THREE CARD TYPES. CARD TYPE 1 IS IN
      (E10.3) FORMAT AND REQUIRES FK1 AND FK2, TWO PRIMARY
      FREQUENCIES IN HZ, P1 AND P2, TWO RMS PRIMARY SOURCE LEVELS
      IN DB RE 1 MICROPAISCAL AT 1 M, A, PISTON RADIUS IN METERS,
      TEMP, WATER TEMPERATURE IN DEGREES CELSIUS, AND S, SALINITY
      IN PARTS PER THOUSAND.

```

```

      CARD TYPE 2 IS IN FORMAT (2I10,2F10.0) AND REQUIRES IJ, A
      CONVERGENCE TEST CONTROL, M, THE RANGE INTEGRATION STEP
      CONTROL, XNM, THE AZIMUTH INTEGRATION STEP CONTROL, AND
      BOVERA, THE PARAMETER OF NONLINEARITY, AND DEPTH THE
      PROJECTOR DEPTH IN METERS. IJ TAKES THE VALUES
      1 AND 2. IF IT IS 1, A CONVERGENCE TEST IS PERFORMED WHICH
      CONSISTS OF ADDING 10 TO THE NUMBER OF RANGE INTEGRATION STEPS
      AND RECOMPUTING SLD. THE DIFFERENCE IS OUTPUT AS DELTA AND IS
      A MEASURE OF THE CONVERGENCE. M IS THE NUMBER OF STEPS IN THE
      RANGE INTEGRATION. XNM IS THE NUMBER OF AZIMUTH STEPS PER
      DEGREE OF MAIN LOBE HALFWIDTH. THE INTEGRATION IS CARRIED OUT
      BETWEEN THE FIRST INFINITIES OF THE PRIMARY BEAM MAIN LOBE.

```

```

      CARD TYPE 3 IS OF FORMAT (E10.3) AND REQUIRES A RANGE IN METERS.

```

```

      A ZERO VALUE FOR FK1 ON CARD TYPE ONE TERMINATES THE PROGRAM.
      OTHERWISE, CARD TYPE 1 IS ALWAYS FOLLOWED BY ONE CARD TYPE 2.
      THEN, AS MANY CARDS TYPE 3 AS DESIRED ARE INPUT. A ZERO
      RANGE SIGNALS A NEW CASE, AND A NEW CARD TYPE 1 IS READ.

```

J. C. LOCKWOOD

17 MAY 1977

```

COMMON A1PA2,BK1(400),COSX(400),SINX(400),R,KD,IFSL,ITIME,OUTR(200CTH00010
+0),OUTI(2000),RO,A,K1,K2,RMAX,ALPHAD,P1,P2,BOVERA,SHRO,SIG,CG , CTHC00P3
1RFL,XYZ,ZU

```

DIMENSION X(34)

REAL K1,K2,KD

REAL JO,J1

DATA X/4HWD ,4H ,4HSM R,4H0 ,4HP1 ,4H ,4HK1 ,4H

\*4HK2 ,4H ,4HA ,4H ,4HRH00,4H ,4HCO ,4H ,4H3/A ,

\*4H ,4HWD,4HTH ,4HKD ,4H ,4HALPH,4HA1 ,4HALPH,4HA2 ,

\*4HP2 ,4H ,4HALPH,4HAD ,4HF1 ,4H ,4HF2 ,4H /

ASINH(X)=ALOG(X+(X\*X+1)\*\*.5)

PI=3.141592 \$ TUPI=2.0\*PI

C THE FOLLOWING STATEMENT READS CARD TYPE 1

999 READ 2,FK1,FK2,P1,P2,A,RH00,TEMP,S

IF (FK1-EQ.0.0)GO TO 12

P1=P1-96.2227

```

CTH00070
CTH00080
CTH00100
CTH00110
CTH00120
CTH00130
CTH00140
CTH00160

```

```

CTH00190
CTH00220

```



```

60      P2=P2-96.2227
        A=A+100.
        RH00=RH00/1000.
        C      THE FOLLOWING STATEMENT READS CARD TYPE 2
        READ 301,I,J,M,XNN,BOVERA,DEPTH
        PRESS=DEPTH*.097+1.
301      FORMAT(2I10,3F10.0)
        NM=M
        FK0=ABS(FK1-FK2)
        WD=TUPI*FK0 & CO=SPEED(S,TEMP,PRESS)
        CO=CO & RMAX=SMRO & RH00=RH00
        K1=TUPI*FK1/CO & K2=TUPI*FK2/CO
        SMRO=(K1+K2)/2.*(A/2.)**2
        KD=TUPI*ABS(FK1-FK2)/CO
        HWIDTH=ASIN(3.83170571/A/(K1+K2)*2.)/.0174533
        ALPHA2=ALF(S,TEMP,FK2/1000.,PRESS)
        ALPHA=ALF(S,TEMP,FK0/1000.,PRESS)
        FORMAT(/,5X,"S = ",F4.1," PPT",5X,"TEMP = ",F5.2," C",5X,/)
2        FORMAT(8E10.3)
        REF=91.44
9        FORMAT("1 PARAMETERS (CONVERTED TO CGS ; P1 AND P2 ARE PEAK RE 1 MI
1        CROBAR AT 1 YD) : ",/,(/,(8X,2A4,2H=,E16.9))
300      FORMAT(7,9X,2HR,29X,2MPD,30X,3MSLD,17X,3HDELTA,20X,1HR,/)
        PRINT 15
13      FORMAT(////)
        PRINT 9,X(1),X(2),WD,X(3),X(4),SMRO,X(5),X(6),P1,
        ?X(27),X(28),P2,X(31),X(32),FK1,X(33),X(34),FK2,
        ?X(7),X(8),K1,X(9),X(10),K2,X(11),X(12),A,X(13),X(14),RH00,
        ?X(15),X(16),CO,X(17),X(18),BOVERA,X(21),X(22),KD,
        ?X(23),X(24),ALPHA1,X(25),X(26),ALPHA2,X(29),X(30),ALPHA0,
        ?X(19),X(20),HWIDTH
        PRINT 401,S,TEMP
        PRINT 300
1      FORMAT(T115,E10.3)
        P1 = 10.0*(P1/20.0)
        P2 = 10.0*(P2/20.0)
        C=-1.0*WD*WD*REF*REF *P1*P2*(1.0+BOVERA*0.5)
        C=C/( 2.0 * RH00*CO**4)
        ALPHA2=ALPHA1+ALPHA2
        ALPHA2=EXP(-ALPHA2)
        T=0.0
        N=HWIDTH*XNN
        J=N/2+28IF(J.NE.N)N=N+1
        D = 0.0174533/XNN
        NP1=N+1
        DO 4 K=1,NP1
            COSX(K)=COS(T)
            SINX(K)=SIN(T)
            IF(SINX(K).NE.0.0)GOTO 31
30      BK1(K)=BK2 =1.0
            GO TO 4
31      CONTINUE
            BARG=K1+A*SINX(K) & BK1(K)=J1(BARG)
            BARG=K2+A*SINX(K) & BK2 =J1(BARG)
            BK1(K)=4.0+BK1(K)*BK2 /(K1+K2+A*A*SINX(K))/SINX(K)
            T=T+D
4

```

Line	Code	Statement	Card Type
115	200	FORMAT(1X,20F5.3)	
	C	THE FOLLOWING STATEMENT READS CARD TYPE 3	
120	100	READ 2,R0	
		R0=R0+100.	
		IF (R0.EQ.0.) GO TO 999	
		M=M	
125	3	IX1 = IJ	
		UMAX=ASINH(R0/2./SMRO)	
		XP=M	
	40	PRINT1,XR	
		DELTA=UMAX/XP	
		U=0.	
		MP1=M+1	
		DO 5 L=1,MP1	
		P=SMRO+2.*SINH(U)	
		IF (L.EQ.MP1) R=R0	
		IFSW=1	
		ITIME=1	
		RADIAN = HWIDTH*0.0174533	
		CALL INTEGR(OUTR(L),0.0,RADIAN ,N)	
		IFSW=2	
		ITIME=1	
		CALL INTEGR(OUTI(L),0.0,RADIAN ,N)	
		U=U+DELTA	
	5	IFSW=3	
		ITIME=1	
		CALL INTEGR(CAR,0.0,UMAX,P)	
		IFSW=4	
		ITIME=1	
		CALL INTEGR(AI,0.0,UMAX,M)	
		AR=AR+C \$ AI=AI+C	
		AB=SQRT(CAR**2+AI**2)	
		ADB=20.-3*ALOG10(AB)+97.	
		IF (IX1.EQ.2) GO TO 8	
	7	IX1=2	
		XLDB=ADB	
		R0=R0/100.	
	70	M=M+10	
		GO TO 40	
	8	DELTA=(XLDB-ADB)	
		XLDB=ADB	
		R0=R0/100.	
		ADB=ADB+20.*ALOG10(R0)	
	10	PRINT 10,R0,AR,AI,ADB,DELTA	
		FORMAT(2X,E16.9,5X,E16.9,3H + ,E16.9,2H I,5X,E16.9,5X,E16.9)	
		GO TO 100	
	12	PRINT 5252	
	5252	FORMAT(1H1)	
		END	



R1706

PAGE 1

77/07/08. 10.52.40

FTR 4.6+428

SUBROUTINE COSIN 73/74 OPT=1

SUBROUTINE COSIN(X,SX,CX)  
SX=SIN(X)  
CX=COS(X)  
RETURN  
END

1

5

77/07/08. 10.52.40

FTN 4.6+428

FUNCTION J1 73/74 OPT=1

```

1      REAL FUNCTION J1(X)
2      T=0.
3      A=0.
4      T=D.
5      Z=X
6      X=ABS(X)
7      IF(X-LE-.3)GO TO 5
8      IF(X-GE.3)GO TO 10
9      GO TO 15
10     S
11     X=Z
12     V=X/3.
13     A=-.56249985*(Y**2)+.21093573*(Y**4)-.03954289*(Y**6)
14     A=(A+.00463319*(Y**8)-.00031761*(Y**10)+.00001109*(Y**12))*X
15     J1=A
16     GO TO 15
17     V=3./X
18     F=.79788456+.00000156*Y+.01559667*(Y**2)+.00017105*(Y**3)
19     F=-.00249511*(Y**4)+.00116553*(Y**5)-.00020033*(Y**6)
20     T=X-2.35619449+.12499612*(Y)+.03005650*(Y**2)-.00637879*(Y**3)
21     T=1+.0007436*(Y**4)+.00079926*(Y**5)-.00029166*(Y**6)
22     J1=F*COS(T)/X**5
23     IF(2-LY-D.)J1=-J1
24     RETURN
25     END

```

CTW01570

J1 00030  
 J1 00040  
 J1 00050  
 J1 00060  
 J1 00070  
 J1 00080  
 J1 00090  
 J1 00100  
 J1 00110  
 J1 00120  
 J1 00130  
 J1 00140  
 J1 00150  
 J1 00160  
 J1 00170  
 J1 00180  
 J1 00190  
 J1 00200  
 J1 00210  
 J1 00220  
 J1 00230  
 J1 00240  
 J1 00250



```

1      FUNCTION FTC(X)
COMMON A1PA2,PK1(400),COSX(400),SINX(400),R,KD,IFSW,ITIME,OUTR(200),CTH01240
*0),OUTI(200),RO,A,K1,K2,EMAY,ALPHAD,P1,P2,BOVERA,SMRO,SIG,CO , CTH01250
19FL,XYZ,D
5      DIMENSION DU*(1000)
REAL KD
REAL K1,K2
GO TO (10,20,30,40) IFSW
10     O=R $ SIG=SIGMA(G)
IF(SINX(ITIME)-GE-.00001) GO TO 12
11     IF(R.NE.RO) GO TO 22
FTC=1.0/RO/(1.+(SIG/2.))**2)
RAD=KD*RO
GO TO 13
22     FTC=DUM(ITIME)=0.0
GO TO 15
12     RAD=SQRT((R**2+RO*RO-2.0*RO*(COSX(ITIME))))
FTC=BK1(ITIME)*EXP(-ALPHAD*RAD)/RAD*SINX(ITIME)/(1.+(SIG/2.))**2)
RAD=KD*(RAD+R)
13     CALL COSIN(RAD,SX,CX)
DUM(ITIME)=FTC*SX
FTC=FTC*CX
GO TO 15
20     FTC=DUM(ITIME)
15     ITIME=ITIME+1
RETURN
30     FUNC=A1PA2*(SMRO*2.*SINX(X))
FTC=OUTR(ITIME)+FUNC*SMRO*2.*COSH(X)
GO TO 15
40     FUNC=A1PA2*(SMRO*2.*SINX(X))
FTC=OUTI(ITIME)+FUNC*SMRO*2.*COSH(X)
GO TO 15
END
CTH01230
CTH01270
CTH01280
CTH01290
CTH01300
CTH01310
CTH01330
CTH01350
CTH01360
CTH01370
CTH01380
CTH01390
CTH01400
CTH01420
CTH01430
CTH01440
CTH01450
CTH01460
CTH01470
CTH01480
CTH01490
CTH01500
CTH01510
CTH01520
CTH01530
CTH01540
CTH01550
CTH01560

```

PAGE 1

77/07/08. 10.52.40

FTN 4.6+428

FUNCTION SPEED 73/74 OPT=1

```

1  FUNCTION SPEED(S,T,P)
    C SOUND SPEED IN CM/SEC
    C S SALINITY IN PARTS PER THOUSAND
    C T TEMP. IN DEGREES C
    C P PRESSURE IN KG/CM**2 1 ATM FOR 6-980 CM/SEC**2
    VT=4.5721*T-4.4532E-2*T**2-2.6045E-4*T**3+7.9851E-6*T**4
    VP=1.60272E-1*P+1.0268E-5*P**2+3.5216E-9*P**3-3.3603E-12*P**4
    VS=1.39799*(S-35)+1.69202E-3*(S-35)**2
    VSTP=(S-35)*(-1.244E-2*T+7.771E-7*T**2+7.7016E-5*P-1.2943E-7*P**2
    12+3.158E-8*P*T+1.579E-9*P*T**2)+P*(-1.8607E-4*T+7.4812E-6*T**2+4.
    15283E-8*T**3)+P**2*(-2.5294E-7*T+1.8563E-9*T**2)-P**3*1.9646E-10*
    SPEED=1449.14+VT+VP+VS+VSTP
    SPEED=SPEED*100.
    RETURN
    END
15

```

ALS00010  
 ALS00020  
 ALS00030  
 ALS00040  
 ALS00050  
 ALS00060  
 ALS00070  
 ALS00080  
 ALS00090  
 ALS00100  
 ALS00110  
 ALS00120  
 ALS00130  
 ALS00140  
 ALS00150



R1706

FTN 4.6+428

77/07/08. 10.52.40

PAGE 1

73/74 OPT=1

FUNCTION E1

```
1      FUNCTION E1(X)
      A=X
      CALL EXPI(RES,A,AUX)
      C      EXPI IS IN THE IBM SCIENTIFIC SUBROUTINE PACKAGE (SSPLIB/UN=RAYFTN)
      E1=RES
      RETURN
      END
```

FUNCTION ALF	73/74	OPT=1	FTN 4.6+428	77/07/38. 10.52.40	PAGE 1
--------------	-------	-------	-------------	--------------------	--------

```

1  FUNCTION ALF(S,T,F,P)
   C  SMALL SIGNAL ABSORPTION COEFFICIENT IN NEPERS/CM
   C  ONE NEPER IS 8.686 DB
   C S - SALINITY IN PARTS/THOUSAND
   C T - TEMP IN DEGREES C
   C F - FREQ IN KHZ
   C P - PRESSURE KG/CM**2 = 1 ATM IF 6=980 CM/SEC**2
      IF(S.GT.0.0) GO TO 1
      A = 6.0 - 1520.0/(T + 273.0)
      FT=21.9+10.0**A
      ALF=((2.34E-6*S*FT*F*F)/(FT*FT*F*F) + 3.38E-6*F*F/FT)*
1  (1.0-6.54E-4*P)
      ALF=ALF/100 $ RETURN
1  A1=1.7760
   A2=32.768
   A3=6.54E-04
   A4=0.018587
   A5=0.026847
   E=2.7182818285
   CF=1.0936133E-05/(20.0+ALOG10(E))
   TEMP=T
   FT=21.9+10.0**((6.0*TEMP+118.0)/(TEMP+273.0))
   FKNZ=F
   FKNZ2=FKNZ*FKNZ
   FKNZ3=FKNZ*FKNZ2
   ALFADB=(A1*FKNZ**1.5/(A2+FKNZ3))+((1.0-A3*P)/(1.0+A2/FKNZ3))*((A4
   **S*FT*FKNZ2/(FKNZ2+FT*FT))+A5*FKNZ2/FT)
   ALF=ALFADB*CF
   RETURN
   END
30

```

ALS00010  
 ALS00020  
 ALS00030  
 ALS00040  
 ALS00050  
 ALS00060  
 ALS00070  
 ALS00080  
 ALS00090  
 ALS00100  
 ALS00110  
 ALS00120  
 ALS00130  
 ALS00140  
 ALS00150  
 ALS00160  
 ALS00170  
 ALS00180  
 ALS00190  
 ALS00200  
 ALS00210  
 ALS00220  
 ALS00230  
 ALS00240  
 ALS00250  
 ALS00260  
 ALS00270  
 ALS00280  
 ALS00290  
 ALS00300



SUBROUTINE INTEGR 73/74 OPT=1

```
1  SUBROUTINE INTEGR(X,BOT,TOP,INT)
   XINT=INT
   H=(TOP-BOT)/XINT
   X=FTC(BOT)
   W=4.D
   5  9=BOT+H
   N=INT-1
   DO 1 K=1,N
   10  A=FTC(B)
   A=A*W
   X=X+A
   B=B+H
   W=6.-W
   1  X=X+FTC(TOP)
   X=X*H/3.
   15  RETURN
   END
```

FUNCTION SIGMA 73/74 OPT=1

```

1      FUNCTION SIGMA(Q)
      C
      C
      C
      MODIFIED BERKTAJ LEAHY SIGMA WITH DIRECTIVITY
      COMMON A1PA2,BK1(400),COSX(400),SINX(400),R,KD,IFSH,ITIME,OUTR(200),
      *O),OUTI(2000),RD,A,K1,K2,SMRD,ALPHAD,P1,P2,BOVERA,RMAX,SIG,CD,
      1RFL,XYZ,D
      REAL K1,K2,KD
      RRAYL=2.*RMAX
      EPS=(P1+P2)/(CD**2)
      BETA=1.+BOVERA/2.
      AK=(K1*K2)/2.
      ALPHO=-ALOG(A1PA2)
      BEK=BETA*EPS*AK*91.44
      IF(Q.GT.RRAYL) GO TO 10
      SIGMA=BEK/(ALPHO*RRAYL)*(1.-EXP(-ALPHO*R))
      RETURN
10     D2=BK1(ITIME)
      IF(D2.LT.0.) D2=-D2
      D=SQRT(D2)
      IF(ITIME.NE.1) GOT01
      SIGMAO=BEK/(ALPHO*RRAYL)*(1.-EXP(-ALPHO*PRAYL))
      X0=ALPHO*RRAYL
      FACT=(E1(X0)-E1(X1))
      SIGMA=FACT*D*BEK*SIGMAO
      RETURN
      END
25     1

```

```

TAP00010
TAP00020
TAP00030
TAP00040
TAP00050
TAP00060
TAP00070
TAP00080
TAP00090
TAP00100
TAP00110
TAP00120
TAP00130
TAP00140
TAP00160
TAP00170
TAP00180
TAP00190
TAP00200
TAP00210
TAP00220
TAP00230
TAP00240
TAP00250
TAP00260
TAP00270
TAP00280
TAP00290

```



## APPENDIX B

In this appendix is supplied for reference a FORTRAN listing of the main program and required subprograms used to evaluate the Lockwood model. A description of the model may be found in Reference 5.

This program has also been implemented on a programmable calculator (Texas Instruments SR-52).

```

1      C
2      C
3      C
4      C
5      C
6      C
7      C
8      C
9      C
10     C
11     C
12     C
13     C
14     C
15     C
16     C
17     C
18     C
19     C
20     C
21     C
22     C
23     C
24     C
25     C
26     C
27     C
28     C
29     C
30     C
31     C
32     C
33     C
34     C
35     C
36     C
37     C
38     C
39     C
40     C
41     C
42     C
43     C
44     C
45     C
46     C
47     C
48     C
49     C
50     C
51     C
52     C
53     C
54     C
55     C
56     C
57     C
58     C
59     C
60     C
61     C
62     C
63     C
64     C
65     C
66     C
67     C
68     C
69     C
70     C
71     C
72     C
73     C
74     C
75     C
76     C
77     C
78     C
79     C
80     C
81     C
82     C
83     C
84     C
85     C
86     C
87     C
88     C
89     C
90     C
91     C
92     C
93     C
94     C
95     C
96     C
97     C
98     C
99     C
100    C
101    C
102    C
103    C
104    C
105    C
106    C
107    C
108    C
109    C
110    C
111    C
112    C
113    C
114    C
115    C
116    C
117    C
118    C
119    C
120    C
121    C
122    C
123    C
124    C
125    C
126    C
127    C
128    C
129    C
130    C
131    C
132    C
133    C
134    C
135    C
136    C
137    C
138    C
139    C
140    C
141    C
142    C
143    C
144    C
145    C
146    C
147    C
148    C
149    C
150    C
151    C
152    C
153    C
154    C
155    C
156    C
157    C
158    C
159    C
160    C
161    C
162    C
163    C
164    C
165    C
166    C
167    C
168    C
169    C
170    C
171    C
172    C
173    C
174    C
175    C
176    C
177    C
178    C
179    C
180    C
181    C
182    C
183    C
184    C
185    C
186    C
187    C
188    C
189    C
190    C
191    C
192    C
193    C
194    C
195    C
196    C
197    C
198    C
199    C
200    C
201    C
202    C
203    C
204    C
205    C
206    C
207    C
208    C
209    C
210    C
211    C
212    C
213    C
214    C
215    C
216    C
217    C
218    C
219    C
220    C
221    C
222    C
223    C
224    C
225    C
226    C
227    C
228    C
229    C
230    C
231    C
232    C
233    C
234    C
235    C
236    C
237    C
238    C
239    C
240    C
241    C
242    C
243    C
244    C
245    C
246    C
247    C
248    C
249    C
250    C
251    C
252    C
253    C
254    C
255    C
256    C
257    C
258    C
259    C
260    C
261    C
262    C
263    C
264    C
265    C
266    C
267    C
268    C
269    C
270    C
271    C
272    C
273    C
274    C
275    C
276    C
277    C
278    C
279    C
280    C
281    C
282    C
283    C
284    C
285    C
286    C
287    C
288    C
289    C
290    C
291    C
292    C
293    C
294    C
295    C
296    C
297    C
298    C
299    C
300    C
301    C
302    C
303    C
304    C
305    C
306    C
307    C
308    C
309    C
310    C
311    C
312    C
313    C
314    C
315    C
316    C
317    C
318    C
319    C
320    C
321    C
322    C
323    C
324    C
325    C
326    C
327    C
328    C
329    C
330    C
331    C
332    C
333    C
334    C
335    C
336    C
337    C
338    C
339    C
340    C
341    C
342    C
343    C
344    C
345    C
346    C
347    C
348    C
349    C
350    C
351    C
352    C
353    C
354    C
355    C
356    C
357    C
358    C
359    C
360    C
361    C
362    C
363    C
364    C
365    C
366    C
367    C
368    C
369    C
370    C
371    C
372    C
373    C
374    C
375    C
376    C
377    C
378    C
379    C
380    C
381    C
382    C
383    C
384    C
385    C
386    C
387    C
388    C
389    C
390    C
391    C
392    C
393    C
394    C
395    C
396    C
397    C
398    C
399    C
400    C
401    C
402    C
403    C
404    C
405    C
406    C
407    C
408    C
409    C
410    C
411    C
412    C
413    C
414    C
415    C
416    C
417    C
418    C
419    C
420    C
421    C
422    C
423    C
424    C
425    C
426    C
427    C
428    C
429    C
430    C
431    C
432    C
433    C
434    C
435    C
436    C
437    C
438    C
439    C
440    C
441    C
442    C
443    C
444    C
445    C
446    C
447    C
448    C
449    C
450    C
451    C
452    C
453    C
454    C
455    C
456    C
457    C
458    C
459    C
460    C
461    C
462    C
463    C
464    C
465    C
466    C
467    C
468    C
469    C
470    C
471    C
472    C
473    C
474    C
475    C
476    C
477    C
478    C
479    C
480    C
481    C
482    C
483    C
484    C
485    C
486    C
487    C
488    C
489    C
490    C
491    C
492    C
493    C
494    C
495    C
496    C
497    C
498    C
499    C
500    C

```

PROGRAM HORN(TAPES, TAPES)  
 THIS PROGRAM CALCULATES THE AXIAL SOURCE LEVEL OF A PARAMETRIC  
 TRANSMITTING ARRAY BY APPLYING GEOMETRICAL CORRECTION FACTORS  
 TO LEVELS BASED ON THE 1971 MELLER-MOFFETT THEORY. A FACTOR  
 IS APPLIED ONLY TO A PORTION OF THE INTERACTION RANGE AND IT IS  
 NECESSARY THAT ATTENUATION IN THIS PORTION BE INSIGNIFICANT IF THE  
 OBSERVATION POINT IS IN THE NEARFIELD.  
 THE INPUTS ARE SO FORMATTED THAT THE SAME INPUT FILE MAY BE  
 USED FOR BOTH WILLET AND HORN. THEREFORE, CERTAIN VARIABLES,  
 SPECIFICALLY IJ, RHO, M, XNM, AND BOVERA, ARE DUMMYS. FOR  
 GENERAL COMPATIBILITY, THE INPUT SHOULD BE PREPARED FOLLOWING THE  
 INSTRUCTIONS FOR WILLET.  
 FK1 AND FK2 ARE IN HZ, SL1 AND SL2 ARE FPS RE 1 MCKOPASCAL AT 1 M, A  
 IS RADIUS IN METERS, TEMP IS IN DEGREES CELSIUS, AND DEPTH IS IN  
 METERS.  
 EXTERNAL FTC  
 COMMON TUARD, DSR, CHI  
 REAL LSD  
 NAMELIST/INPUTS/(FK1,FK2,SL1,SL2,A,RHO,TEMP,S  
 ARSINH(X)=ALOG(X+(X\*X+1)\*\*.5)  
 PI=3.14159265  
 READ(5,2)FK1,FK2,SL1,SL2,A,RHO,TEMP,S  
 IF(FK1.EQ.0)GO TO 12  
 READ(5,301)IJ,M,XNM,BOVERA,DEPTH  
 PRESS=DEPTH\*.097+1.  
 WRITE(6,INPUTS)  
 FORMAT(8E10.3)  
 FOOVF=(FK1+FK2)/ABS(FK1-FK2)/2.  
 FO=(FK1+FK2)/2./1000.  
 ALPHA=ALF(S,TEMP,FO,PRESS)  
 CO=SPEED(S,TEMP,PRESS)/100.  
 RO=(FK1+FK2)\*2.\*PI/CO\*(A/2)\*\*2  
 RO=RO/.9144  
 SPL=(SL1+SL2)/2.-96.2227  
 FORMAT(2I10,3F10.0)  
 CO=CO\*100.  
 READ(5,102) R  
 FORMAT(F11.4)  
 IF(R.EQ.0.)GO TO 999  
 R=R/.9144  
 DSR=1./FOOVF  
 TUARD=2.\*RO\*91.44\*ALPHA  
 UMAX=ARSINH(R/RO)  
 EPS=10.\*\*((SPL/20.)/CO/CC  
 AK=3.83\*FO  
 CHI=3.5\*EPS\*AK  
 USMRD=ARSINH(FOOVF)  
 CALL FACTOR(FAC,ICASE,R,RO,FOOVF)  
 IF(ICASE.LE.2) GO TO 500  
 CALL INTGR(FTC,ROINT,D.,UMAX,30)  
 UTST=UMAX  
 PE=FAC\*ROINT\*CHI/2.\*DSR\*DSR  
 EXINT=D.  
 GO TO 600  
 CALL INTGR(FTC,ROINT,D.,US\*RO,30)

NF100320  
NF100330

NF100040  
NF100050

NF100070

NF100390  
NF100100

NF100110  
NF100120

NF100140  
NF100150

NF100160  
NF100190

NF100210  
NF100220

NF100230  
NF100240

NF100250  
NF100260

NF100270  
NF100280

NF100290  
NF100300

NF100310  
NF100320

NF100330  
NF100340

NF100350  
NF100360

NF100370



77/07/38. 10.48.41

FTN 4.6+428

73/74 OPT=1

PROGRAM HORN

```

60      UTST=USMRO
        CALL INTGR(FIC,EXINT,USMRO,UMAX,30)
        PE=(FAC*ROINT+EXINT)*CHI/2.*DSR*DSR
        CONTINUE
        SPLD=SPL-20.*ALOG10(R)+20.*ALOG10(PE)+97.
        CHI=1.E-4
        TUARO=1.E-4
65      CALL INTGR(FIC,ISTINT,J,UTST,30)
        IF(TSTINT/ROINT.GE..89.5C.FAC.LT.1.27) GO TO 103
        WRITE(6,110)
110      FORMAT("WARNING: SIGNIFICANT ATTENUATION IN REGION TO WHICH FACTOR
        11S APPLIED")
70      R=R*.9144
        SPLD=SPLD+20.*ALOG10(R)
        PE=20.*ALOG10(PE)
        WRITE(6,109) R,SPLD,PE
75      FORMAT(" R=",F11.4,"SLD=",F11.4,"PARAMETRIC EFFICIENCY=",F11.4)
        WRITE(6,112)P,ICASE,FAC
        FORMAT("R=",F11.4,"ICASE=",I1,"FAC=",F11.4)
        GO TO 100
12      CONTINUE
        END

```

NF100380  
NF100390  
NF100400  
NF100410

NF100420  
NF100430

NF100470  
NF100480  
NF100490  
NF100500

FUNCTION FTC	73/74	OPT=1	FTN 4.6*428	77/07/DP. 10.4P.41	PAGE	1
1	<pre> FUNCTION FTC(U) COMMON TUARO,DSR,CHI A=SINH(U) B=DSR*A C=-TUARO*A D=CHI*U/2. FTC=EXP(C)/(1.+D**2) FTC=FTC*SQR(1.+A*A)/(1.+B*B) RETURN END </pre>					
5						
10	<pre> FTC00010 FTC00020 FTC00030 FTC00040 FTC00050 FTC00060 FTC00070 FTC00080 FTC00090 FTC00100 </pre>					



77/07/38. 10.48.41

FTN 4.6+428

7374 OPT=1

FUNCTION ALF

```

1  FUNCTION ALF(S,T,F,P)
    C  SMALL SIGNAL ABSORPTION COEFFICIENT IN NEPERS/CM
    C  ONE NEPER IS 8.686 DB
    C  S - SALINITY IN PARTS/THOUSAND
    C  T - TEMP IN DEGREES C
    C  F - FREQ IN KHZ
    C  P - PRESSURE KG/CM**2 = 1 ATM IF 6=980 CM/SEC**2
    IF(S.GT.0.0) GO TO 1
    A = 6.0 - 1520.0/( T + 273.0 )
    FT=21.9*10.0**A
    ALF=((2.34E-6*S*FT*F*F)/(FT*FT*F*F) + 3.38E-6*F*F/FT)*
    1 (1.0-6.54E-4*P)
    ALF=ALF/100 $ RETURN
1  A1=1.7760
    A2=32.768
    A3=6.54E-04
    A4=0.018587
    A5=0.026847
    E=2.7182818285
    CF=1.0936133E-05/(20.0*ALOG10(E))
    TEMP=T
    FT=21.9*10.0**((6.0*TEMP+118.0)/(TEMP+273.0))
    FKNZ=F
    FKNZ2=FKNZ*FKNZ
    FKNZ3=FKNZ*FKNZ2
    ALFADB=(A1*FKNZ**1.5/(A2*FKNZ3))+((1.0-A3*P)/(1.0+A2/FKNZ3))*((A4
    *S*FT*FKNZ2/(FKNZ2*FT*F))+A5*FKNZ2/FT)
    ALF=ALFADB*CF
    RETURN
    END
30

```

ALS00010  
 ALS00020  
 ALS00030  
 ALS00040  
 ALS00050  
 ALS00060  
 ALS00070  
 ALS00080  
 ALS00090  
 ALS00100  
 ALS00110  
 ALS00120  
 ALS00130  
 ALS00140  
 ALS00150  
 ALS00160  
 ALS00170  
 ALS00180  
 ALS00190  
 ALS00200  
 ALS00210  
 ALS00220  
 ALS00230  
 ALS00240  
 ALS00250  
 ALS00260  
 ALS00270  
 ALS00280  
 ALS00290  
 ALS00300

77/07/38. 10.48.41

FTN 4.6+428

SUBROUTINE INTGRT 73/74 OPT=1

```

1      SUBROUTINE INTGRT(FTC,X,BOT,TOP,INT)
      C*****27 MARCH 1975*****
      EXTERNAL FTC
      XINT=INT
      N=(TOP-BOT)/XINT
      X=FTC(BOT)
      W=4.
      B=BOT+H
      N=INT-1
      DO 1 K=1,N
      A=FTC(S)
      A=A+W
      X=X+A
      B=B+H
      W=6.-W
      X=X+FTC(TOP)
      X=X+H/3.
      RETURN
      END
10
15

```

```

CIN03310
CIN00020
CIN03330
CIN00040
CIN00050
CIN03360
CIN00070
CIN03380
CIN03390
CIN00100
CIN03110
CIN00120
CIN03130
CIN03140
CIN03150
CIN03160
CIN03170
CIN03180
CIN03190

```



SUBROUTINE FACTOR 73/74 OPT=1

```

1  SUBROUTINE FACTOR(FAC, ICASE, R, RO, FOOVF)
    ROMIN=RO/FOOVF
    SMRO=RO*FOOVF
    RC=(SMRO/2.)*(-1.+SQRT(1.+4.*R/SMRO))
    IF(R-6E-2.*SMRO) ICASE=1
    IF(R-LT-2.*SMRO) ICASE=2
    IF(R-LT-SMRO) ICASE=3
    IF(R-LT-RO+ROMIN) ICASE=4
    IF(R-LT-RO) ICASE=5
    IF(R-LT-ROMIN) ICASE=6
    GO TO (10,20,30,40,50,60), ICASE
    FAC=R/SMRO*ALOG(R/(R-SMRO))
    RETURN
10  FAC=R/SMRO*(ALOG(R/(R-RC))+(SMRO-RC)/RC)
    RETURN
15  FAC=ALOG(R/(R-RC))+SMRO/R*(R-RC)/RC
    RETURN
20  FAC=ALOG(R/ROMIN)-(R-RO)**2/R/ROMIN+1.
    RETURN
    FAC=ALOG(R/ROMIN)+1.
    RETURN
    FAC=R/ROMIN
    RETURN
    END

```

77/07/08. 10.48.41

FTN 4.6+428

FUNCTION SPEED 73/74 OPT=1

```

1      FUNCTION SPEED(S,T,P)
      C SOUND SPEED IN CM/SEC
      C S SALINITY IN PARTS PER THOUSAND
      C T TEMP. IN DEGREES C
      C P PRESSURE IN KG/CM**2 1 ATM FOR G=980 CM/SEC**2
      VT=4.5721*T-4.4532E-2*T**2-2.6045E-4*T**3+7.9851E-6*T**4
      VP=1.60272E-1*P+1.0268E-5*P**2+3.5216E-9*P**3-3.3603E-12*P**4
      VS=1.39799*(S-35)+1.69202E-3*(S-35)**2
      VSTP=(S-35)*(-1.244E-2*T+7.7711E-7*T**2+7.7016E-5*P-1.2943E-7*P**2+
12+3.158E-8*P*T+1.579E-9*P*T**2)+P*(-1.6607E-4*T+7.4812E-6*T**2+6.
15283E-8*T**3)+P**2*(-2.5294E-7*T+1.8563E-9*T**2)-P**3+1.9646E-10*
      SPEED=1449.14+VT+VP+VS+VSTP
      SPEED=SPEED*100.
      RETURN
      END
15

```

```

ALSO0010
ALSO0020
ALSO0030
ALSO0040
ALSO0050
ALSO0060
ALSO0070
ALSO0080
ALSO0090
ALSO0100
ALSO0110
ALSO0120
ALSO0130
ALSO0140
ALSO0150

```